

Topology optimization of load-carrying structures using three different types of finite elements

S H O A I B A H M E D

Master of Science Thesis
Stockholm, Sweden 2013

Topology optimization of load-carrying structures using three different types of finite elements

S H O A I B A H M E D

Master's Thesis in Optimization and Systems Theory (30 ECTS credits)
Master Programme in Mathematics (120 credits)
Royal Institute of Technology year 2013
Supervisor at KTH was Krister Svanberg
Examiner was Krister Svanberg

TRITA-MAT-E 2013:35
ISRN-KTH/MAT/E--13/35--SE

Royal Institute of Technology
School of Engineering Sciences

KTH SCI
SE-100 44 Stockholm, Sweden

URL: www.kth.se/sci

Abstract

This thesis deals with topology optimization of load-carrying structures, in particular compliance minimization subject to a constraint on the total amount of material to be used.

The main purpose of the work was to compare the following three types of finite elements for the above topology optimization problems: Four node square elements with bilinear shape functions, nine node square elements with quadratic shape functions, and six node hexagonal elements with Wachspress shape functions.

The SIMP approach (Solid Isotropic Material with Penalization) was used to model the topology optimization problem for different load and support conditions, and the method of moving asymptotes (MMA) was used to solve the formulated optimization problems.

On the considered test problems, it turned out that the results obtained by using six node hexagonal elements were in general better than the corresponding results using nine node square elements which in turn were better than the results using four node square elements. The price paid for the improvements were increased computation times.

Acknowledgment

All prays be to Almighty ALLAH, the most gracious, compassionate and ever merciful WHO has given me knowledge, power and strength to accomplish this task.

I am extremely thankful to my Supervisor, Krister Svanberg under whose patronage, supervision and guidance; I carried out my research work successfully and achieved the goal. His diversified experience, in-depth knowledge and command on the subject benefited me a lot. It was a great opportunity for me to do Master thesis under his able guidance and supervision. I will never forget his generous and affectionate help.

Last but not the least, I pay my sincere thanks to my parents whose prayers continually shielded me in all of my life. They always supported me particularly, in a difficult time and encouraged me to move forward. I am also thankful to my brothers and sisters, specially my eldest sister and younger brother for their affection, assistance and prayers.

For further information regarding the contents of this technical report, please contact the author: shoaibah@kth.se; shoaib.ciit@gmail.com or the Department of Optimization and Systems Theory, KTH, Stockholm, Sweden.

Shoaib Ahmed

June 13, 2013.

Contents

List of Figures

List of Tables

1	Introduction	1
1.1	Topology optimization	2
1.2	Finite element method	4
2	Topology optimization problem for compliance minimization	7
2.1	Introduction	7
2.2	Topology optimization model	7
2.3	Optimality criteria	8
2.4	Mesh-independency filter	9
2.5	Method of moving asymptotes	10
2.6	Topology optimization problems	11
2.6.1	Half MBB beam	12
2.6.2	Short cantilever beam	13
2.6.3	Cantilever beam with a fixed hole	14
2.7	Continuation procedure	15
2.8	Results and Discussion	15
2.8.1	MBB beam	15
2.8.2	Short cantilever beam	15
2.8.3	Cantilever beam with a fixed hole	17
3	Comparison of SIMP model and alternative model	19
3.1	Introduction	19
3.2	SIMP model	19
3.3	Alternate model	20

CONTENTS

3.4	Results and Discussion	21
3.4.1	MBB beam	21
3.4.2	Short cantilever beam	22
3.4.3	Cantilever beam with a fixed hole	22
4	Four node square elements, nine node square elements and six node hexagonal elements	25
4.1	Introduction	25
4.2	Finite elements used	25
4.3	Four node square element	26
4.4	Nine node square element	26
4.5	Six node hexagonal element	27
4.6	Results and Discussion	28
4.6.1	40% Volume	31
4.6.2	50% Volume	36
4.7	Another load condition	42
4.7.1	40% Volume - 80×80	42
4.7.2	50% Volume - 80×80	46
5	Conclusion and future work	49
5.1	Conclusion	49
5.2	Recommendations for future work	50
A	Finite element method procedure	51
A.1	Domain discretization	51
A.2	Displacement interpolation:	51
A.2.1	Local and Global coordinates	52
A.3	Construction of shape function:	52
A.3.1	Properties of shape function	53
A.4	Formation of FE equations in local coordinate system	54
B	Shape functions	55
B.1	Four node square element	55
B.2	Nine node square element	56
B.3	Six node hexagonal elements	56
C	Gauss integration	57
C.1	Four node element and nine node element	57

C.2 Six node element	58
D Hexagonal element	61
Bibliography	63

List of Figures

2.1	Topology optimization problems	12
2.2	Half MBB beam solved by OC on left and MMA on right	13
2.3	Short cantilever beam solved by OC on left and MMA on right	13
2.4	Cantilever beam with a fixed hole solved by OC on left and MMA on right	14
2.5	Half MBB beam solved by continuation procedure with MMA	16
2.6	Short cantilever beam solved by continuation procedure with MMA . .	16
2.7	Cantilever beam with a fixed hole solved by continuation procedure with MMA	17
3.1	Half MBB beam solved with alternate model	23
3.2	Short cantilever beam solved with alternate model	23
3.3	Cantilever beam with a fixed hole solved with alternate model	23
4.1	The finite element four node in local coordinates (ξ, η)	27
4.2	The finite element nine node in local coordinates (ξ, η)	28
4.3	Square element mesh can display one node-connection while hexagonal mesh shows two node-connection	29
4.4	The square element has two edges-based-symmetry lines whereas hexagonal element has three edge-based symmetry lines	29
4.5	Design domain, loads and support for square element (a) and hexagonal element (b)	30
4.6	Four node square elements without filter; Volume 40%, $N = 60 \times 60$. .	32
4.7	Four node square elements with filter; Volume 40%, $N = 60 \times 60$	32
4.8	Nine node square elements; Volume 40%, $N = 60 \times 60$	33
4.9	Six node hexagonal elements; Volume 40%, $N = 60 \times 60$	33
4.10	Four node square element without filter; Volume 40%, $N = 80 \times 80$. . .	34
4.11	Four node square element with filter; Volume 40%, $N = 80 \times 80$	35

List of Figures

4.12 Nine node square element; Volume 40%, $N = 80 \times 80$	35
4.13 Six node hexagonal element; Volume 40%, $N = 80 \times 80$	36
4.14 Four node square elements without filter; Volume 50%, $N = 60 \times 60$. .	37
4.15 Four node square elements with filter; Volume 50%, $N = 60 \times 60$. . .	37
4.16 Nine node square elements; Volume 50%, $N = 60 \times 60$	38
4.17 Six node hexagonal elements; Volume 50%, $N = 60 \times 60$	38
4.18 Four node square elements without filter; Volume 50%, $N = 80 \times 80$. .	39
4.19 Four node square elements with filter; Volume 50%, $N = 80 \times 80$. . .	40
4.20 Nine node square elements; Volume 50%, $N = 80 \times 80$	40
4.21 Six node hexagonal elements; Volume 50%, $N = 80 \times 80$	41
4.22 Four node square elements without filter; Volume 40%, $N = 80 \times 80$. .	43
4.23 Four node square elements with filter; Volume 40%, $N = 80 \times 80$. . .	44
4.24 Nine node square elements; Volume 40%, $N = 80 \times 80$	44
4.25 Six node hexagonal elements; Volume 40%, $N = 80 \times 80$	45
4.26 Four node square elements without filter; Volume 50%, $N = 80 \times 80$. .	46
4.27 Four node square elements with filter; Volume 50%, $N = 80 \times 80$. . .	47
4.28 Nine node square elements; Volume 50%, $N = 80 \times 80$	47
4.29 Six node hexagonal elements; Volume 50%, $N = 80 \times 80$	48
C.1 Schematic illustration of the quadrature rule for the regular hexagonal element	59
D.1 Coordinates for hexagonal element	61
D.2 Six node hexagonal element; $N = 2 \times 2$	62

List of Tables

3.1	Half MBB beam with alternate model and SIMP model	22
3.2	Short cantilever beam with alternate model and SIMP model	22
3.3	Cantilever beam with a fixed hole with alternate model and SIMP model	22
4.1	Volume 40%, Number of elements 60×60	31
4.2	Volume 40%, Number of elements 80×80	34
4.3	Volume 50%, Number of elements 60×60	36
4.4	Volume 50%, Number of elements 80×80	39
4.5	Volume 40%, Number of elements 80×80	43
4.6	Volume 50%, Number of elements 80×80	46
C.1	Gauss integration points and weight coefficients for square elements . .	58
C.2	Quadrature parameters	58
C.3	Gauss integration points for hexagonal element and weight coefficients .	59

Chapter 1

Introduction

This thesis consists of an introduction, four other chapters, list of references and appendices. The purpose of the introduction is to give an overview of the field of topology optimization.

- **Chapter 2,** consists of two parts. In the first part, the SIMP (Solid Isotropic Material with Penalization) approach for compliance minimization is described. This description is mainly based on Sigmund O [19] article, "A 99 line topology optimization code written in Matlab". In the second part, two different optimization methods are compared for SIMP problems. These are optimality criteria method (OC) and method of moving asymptotes (MMA).
- **In chapter 3,** an alternative interpolation scheme for minimum compliance topology is compared with SIMP model.
- **In chapter 4,** the topology optimization problem for minimum compliance is solved using four node square elements (with and without filter), nine node square elements and six node hexagonal elements. The purpose of using higher order element is to hopefully avoid checkerboard patterns that appear when using four node element without filter. Solution obtained with different types of finite elements are compared.
- **Chapter 5,** concludes the report and mention recommendations for future work.
- **Appendices,** includes finite element method procedure, shape functions and Gauss integration for the considered three types of finite elements and also some additional description on hexagonal element.
- **Bibliography,** provides a list of previous work cited in this thesis.

1.1 Topology optimization

Topology optimization is the branch of *structural optimization* that optimizes the layout of a specified amount of material in a selected design domain, for a given set of loads and boundary conditions.

The use of topology optimization can be seen in a variety of different fields like mathematics, mechanics, multi-physics and computer science, but also have important practical applications in the manufacturing (in particular, car, aeronautics, aerospace, building, textile, machine and packing) industries, micro- and nanotechnologies.

In literature there are multiple approaches used by researcher to solve topology optimization problems. Bendøse MP and Kikuchi N [3]; used micro-structure or homogenization approach. Another approach SIMP (Solid Isotropic Material with Penalization) is used by Bendøse MP [1]; Zhou M and Rozvany GIN [30]; Mlejnek HP [14]. An alternative approach to solve minimum compliance topology optimization problem is used by Stolpe M and Svanberg K [21]. Topology optimization has emerged as a powerful and robust tool for the design of structures but still there are problems on numerical issues such as the checkerboard pattern [6]. *Checkerboard* regions are those regions of alternating solid and void elements ordered in a checkerboard fashion. It is undesirable to have a checkerboard pattern in a topology solution because it has artificially high stiffness, and also such a configuration would be difficult to manufacture [16].

Using the objective function and constraints, topology optimization determines the optimum size, shape and topology of the structure. It has been implemented through the use of finite element methods for the analysis, and optimization techniques based on the Optimality Criteria (OC) methods, Method of Moving Asymptotes (MMA), Genetic Algorithm, Sequential Linear Programming (SLP) etc. In this thesis particularly, we focused on optimality criteria method and method of moving asymptotes. Rozvany GIN; Zhou M and Gollub [17]; have studied the general aspects of iterative continuum-based optimality criteria method. Svanberg K [24]; developed method of moving asymptotes.

In *Sizing optimization* problems, the design's geometry (shape) and topology

1.1. TOPOLOGY OPTIMIZATION

are kept constant while modifying specific dimensions of the design. Examples of sizing optimization include the calculation of an optimum cylinder wall thickness, truss-member cross-section area etc.

Shape optimization performs optimization by holding a design's topology constant while modifying the design's shape. For example the determination of the optimum node locations in 10-bar truss, or optimum shape of a rod in tension etc.

Topology optimization performs optimization by modifying the topology of a design. Hence, the design variables control the design's topology, and the values of the design variables define the particular topology of the design. Optimization therefore occurs through the determination of the design variable values which correspond to the component topology providing optimal structural behavior [5]. It is observed that in topology optimization, both the shape of the exterior boundary and configuration of the interior boundaries (i.e. holes) may optimized all at once. Thus sizing and shape optimization occurs as an incidental byproducts of the topology optimization process. The differences between these three structural optimization categories mainly consist of the definition of design variables.

In the so called ground structure approach for topology optimization the design is discretized into small elements, where each element is controlled by a design variable which allowed to attain values between 0 and 1, and the intermediate values should then be penalized. When a particular design variable has a value 0, the corresponding element is assumed to be a void (no material). And when design variable is equal to 1 its corresponding element contains fully-dense material to obtain a "black and white" design. In topology optimization problems it is always favorable to use uniform mesh. For uniform meshes, the constant element density implementation using SIMP model requires the computation of the element stiffness matrix only once.

All optimization problems in this thesis are defined for load carrying structures that are independent of the z-coordinate and applied in the x-y plane. The material is assumed to be isotropic, that is, the material is not direction dependent. The two commonly used material constants are the Young's modulus E and the Poisson's ratio ν . In our study we worked on plane stresses for 2-dimensional solids. The generalized Hook's law written as: $\sigma = \mathbf{c} \varepsilon$, where σ is the stress vector, ε is the

strain vector and \mathbf{c} is a matrix of material constants [29]. In 2-dimensional solids, plane stress, isotropic materials, the relation become:

$$\sigma = \begin{pmatrix} \sigma_{xx} \\ \sigma_{yy} \\ \sigma_{xy} \end{pmatrix} = \mathbf{c} \varepsilon = \frac{E}{1-\nu^2} \begin{bmatrix} 1 & \nu & 0 \\ \nu & 1 & 0 \\ 0 & 0 & \frac{1-\nu}{2} \end{bmatrix} \begin{pmatrix} \varepsilon_{xx} \\ \varepsilon_{yy} \\ \varepsilon_{xy} \end{pmatrix} \quad (1.1)$$

where $\sigma^T = \{\sigma_{xx}, \sigma_{yy}, \sigma_{xy}\}$ are the three stress components called stress tensor, σ_{xy} is the shear stress and $\varepsilon^T = \{\varepsilon_{xx}, \varepsilon_{yy}, \varepsilon_{xy}\}$ are the three strain components and ε_{xy} is the shear strain.

In the iterative solution of the topology optimization problems checkerboard pattern appeared when solved with four node square elements. In order to avoid such patterns the feasible alternates are to use some filtering technique or to use higher order elements like nine node square elements and six node hexagonal elements. Talischi C; Paulino GH and Le CH [26]; worked on six node hexagonal element (honeycomb) with Wachspress shape functions. Wachspress EL [27]; was the first who introduced general interpolants for convex polygon. His work provided a basis for finite element formulations. Later on Wachspress interpolants were developed using the concepts of projective geometry, lowering the order of functions that satisfy the conditions of boundedness, linear precision, and global continuity by Warren J [28]; Sukumar N and Malsch EA [23]. Topology optimization with honeycomb meshes has also been explored by Saxena R and Saxena A [18]; Langelaar M [10].

1.2 Finite element method

Finite Element Method (FEM) is a numerical method seeking an approximated solution of the distribution of field variables, like the displacement in stress analysis, in the problem domain. It is done by dividing the problem domain into many smaller bodies or units (called finite elements) formed by nodes (or nodal point). A *node* is a specific point in the finite element at which the value of the field variable is to be explicitly calculated. The values of the field variable computed at the nodes are used to approximate the values at non-nodal points (i.e., in the element interior) by interpolation of the nodal values. A continuous function of an unknown field variable

1.2. FINITE ELEMENT METHOD

(e.g., displacements) is approximated in each sub-domain. The unknown variables are the values of the field variable at nodes. Then equations are established for the elements, after which the elements are tied to one another. This process leads to a set of linear algebraic simultaneous equations for the entire system that can be solved to yield the required field variable (e.g., strains and stresses) [11]. For detail procedure of finite element method see Appendix A.

Chapter 2

Topology optimization problem for compliance minimization

2.1 Introduction

This chapter comprises on two major parts. In the first part, SIMP approach for compliance minimization of statically loaded structure is described. This description is mainly based on Sigmund O [19] article; "A 99 line topology optimization code written in Matlab". In the second part SIMP model based problems are solved and compared by using two different optimality techniques. The optimality criteria based optimizer is good only for a single constraint and it is based on heuristic fixed point type updating scheme. So a more general optimality technique, namely, method of moving asymptotes (MMA) developed by Svanberg K [24]; is used which solves more complex problems.

2.2 Topology optimization model

A rectangular design domain is assumed and discretized by square finite element mesh defined by n_x , which is the set of elements in the x-axis and n_y , which is the set of elements in the y-axis. In the problem to follow, the design domain is discretized by finite elements, bi-linearly interpolated linear elastic four node membrane elements with two degrees of freedom per node.

The minimum compliance of structure selected as the objective function of the

CHAPTER 2. TOPOLOGY OPTIMIZATION PROBLEM FOR COMPLIANCE
MINIMIZATION

topology optimization problem written as:

$$\begin{aligned} \min_{\mathbf{x}} : c(\mathbf{x}) &= \mathbf{F}^T \mathbf{U}(\mathbf{x}) \\ \text{subject to : } &\sum_{e=1}^N x_e \leq f \cdot N, \quad f \in (0, 1] \\ &0 < \mathbf{x}_j^{min} \leq \mathbf{x}_j \leq 1, \quad j = 1, \dots, n \end{aligned} \quad (2.1)$$

where c is the compliance, \mathbf{F} is a given load vector, $\mathbf{U}(\mathbf{x})$ is the global displacement vector which is obtained as the solution to the system $\mathbf{K}(\mathbf{x})\mathbf{U} = \mathbf{F}$, where $\mathbf{K}(\mathbf{x})$ is the global stiffness matrix. $\mathbf{K}(\mathbf{x})$ is constructed from the local elemental stiffness matrices $\mathbf{k}_e(x_e)$, which are of the form $\mathbf{k}_e(x_e) = E(x_e)\mathbf{k}_0$, where

$$E(x_e) = E_0 + x_e^p(E_1 - E_0) = \begin{cases} E_1 & \text{if } x_e = 1, \\ E_0 & \text{if } x_e = 0, \end{cases}$$

where E_0 and E_1 are the Young moduli and it is assumed that $E_1 > E_0 > 0$ and p is a penalty factor to prevent intermediate densities, which varies between [1, 3] in general. The elemental design variable, x_e , is the relative density of the material in the element and \mathbf{x} is the vector with densities of all the elements. \mathbf{x}^{min} is a non-zero vector of minimum relative densities to avoid singularity, N is the number of elements used to discretize the design domain and keep the distribution of the material limited. $V(\mathbf{x}) = \sum_{e=1}^N x_e$ is the material volume. And f is the allowable volume fraction. It is the ratio between the volume of material to be distributed and the volume of the total design domain.

2.3 Optimality criteria

The optimization problem (2.1) is solved in [19]; by Optimality Criteria (OC) methods. The optimality criteria methods use an iterative redesign algorithm to generate the component design which satisfies a set of optimality criteria defining the structural behavior required for optimality. It is a heuristic updating scheme for the design variables used by Bendøse MP [2]. The method is formulated as:

$$x_e^{new} = \begin{cases} \max(x_{min}, x_e - m) & \text{if } x_e B_e^\eta \leq \max(x_{min}, x_e - m), \\ x_e B_e^\eta & \text{if } \max(x_{min}, x_e - m) < x_e B_e^\eta < \min(1, x_e + m), \\ \min(1, x_e + m) & \text{if } \min(1, x_e + m) \leq x_e B_e^\eta. \end{cases}$$

2.4. MESH-INDEPENDENCY FILTER

where $B_e = -\frac{\partial c}{\partial x_e}$, m is a move-limit, η ($=1/2$) is a numerical damping coefficient to stabilize the iteration, λ is a Lagrangian multiplier chosen in such a way that the volume constraint is satisfied.

The gradient of the objective function c is given by:

$$\frac{\partial c}{\partial x_e} = -p(x_e)^{p-1} \mathbf{u}_e^T \mathbf{k}_0 \mathbf{u}_e \quad (2.2)$$

2.4 Mesh-independency filter

Mesh dependence refers to the problem of not finding the same solution when the domain is discretized using different mesh densities. Although all finite element based solutions have mesh dependency, in some gradient-based methods (i.e., SIMP) the filtering scheme is used in order to avoid the formation of checkerboard patterns [6]; [9]; [20]; to ensure the existence of solutions to the considered topology optimization problem. Here the mesh-independency filter works by modifying the element gradients $\partial c / \partial x_e$ as follows:

$$\widehat{\frac{\partial c}{\partial x_e}} = \frac{1}{x_e \sum_{f=1}^N \hat{H}_{ef}} \sum_{f=1}^N \hat{H}_{ef} x_f \frac{\partial c}{\partial x_f}, \quad (2.3)$$

The convolution operator (weight factor) \hat{H}_{ef} is written as:

$$\begin{aligned} \hat{H}_{ef} &= r_{min} - \text{dist}(e, f), \\ \{f \in N \mid \text{dist}(e, f) \leq r_{min}\}, \quad e &= 1, 2, \dots, N \end{aligned} \quad (2.4)$$

where N is the total number of elements in the mesh and the operator $\text{dist}(e, f)$ is defined as the distance between center of element e and center of element f . The convolution operator \hat{H}_{ef} is zero outside the filter area. The convolution operator decays linearly with the distance from element f . Instead of the original gradients, the modified gradients (2.3) are used [4]; [19].

2.5 Method of moving asymptotes

The Method of Moving Asymptotes (MMA) [24]; is a method for structural optimization problems based on a special type of convex approximation. In each step of the iterative process a approximating convex subproblem is generated and solved. Svanberg's MMA codes [25]; are used to solve the following:

$$\begin{aligned}
 \min_{x,y,z} : & f_0(x) + a_0 z + \sum_{i=1}^m (c_i y_i + \frac{1}{2} d_i y_i^2) \\
 \text{subject to : } & f_i(x) - a_i z - y_i \leq 0, \quad i = 1, \dots, m \\
 & x_j^{\min} \leq x_j \leq x_j^{\max}, \quad j = 1, \dots, n \\
 & y_i \geq 0, \quad i = 1, \dots, m \\
 & z \geq 0
 \end{aligned} \tag{2.5}$$

Here m is the number of constraints, n is the number of elements, f_0, f_1, \dots, f_m are continuously differentiable, real-valued functions. x_j^{\min} and x_j^{\max} are real numbers such that $x_j^{\min} < x_j^{\max}$ for all j . a_0 and a_i are real numbers such that $a_0 > 0$ and $a_i \geq 0$ for all i . c_i and d_i are real numbers such that $c_i \geq 0, d_i \geq 0$, and $c_i + d_i > 0$ for all i . For the given optimization problem (2.1) it is:

$$\begin{aligned}
 \min_x : & f_0(x) \\
 \text{subject to : } & f_i(x) \leq 0, \quad i = 1, \dots, m \\
 & x_j^{\min} \leq x_j \leq x_j^{\max}, \quad j = 1, \dots, n
 \end{aligned} \tag{2.6}$$

Here f_0 is the objective function and f_i are the constraints, with $a_0 = 1, a_i = 0, c_i = 1000$ and $d = 0$ (suggested by Svanberg K). The subproblem at iteration k is as follows:

$$\begin{aligned}
 \min_{\mathbf{x}} : & f_0^{M,k}(\mathbf{x}) \\
 \text{subject to : } & f_i^{M,k}(\mathbf{x}) \leq 0, \quad i = 1, \dots, m \\
 & \alpha_j^k \leq x_j \leq \beta_j^k, \quad j = 1, \dots, n
 \end{aligned}$$

where

$$f_i^{M,k}(\mathbf{x}) = f_i(\mathbf{x}^k) - \sum_{j=1}^n \left(\frac{p_{ij}^k}{U_j^k - x_j^k} + \frac{q_{ij}^k}{x_j^k - L_j^k} \right) + \sum_{j=1}^n \left(\frac{p_{ij}^k}{U_j^k - x_j} + \frac{q_{ij}^k}{x_j - L_j^k} \right),$$

Here, L_j^k and U_j^k are moving asymptotes that satisfy $L_j^k < x_j^k < U_j^k$,

2.6. TOPOLOGY OPTIMIZATION PROBLEMS

$$p_{ij}^k = \begin{cases} (U_j^k - x_j^k)^2 \partial f_i(\mathbf{x}^k) / \partial x_j & \text{if } \partial f_i(\mathbf{x}^k) / \partial x_j > 0 \\ 0 & \text{otherwise,} \end{cases}$$

$$q_{ij}^k = \begin{cases} 0 & \text{if } \partial f_i(\mathbf{x}^k) / \partial x_j \geq 0 \\ -(x_j^k - L_j^k)^2 \partial f_i(\mathbf{x}^k) / \partial x_j & \text{otherwise,} \end{cases}$$

while α_j^k and β_j^k are move limits.

The MMA call is

```
function[xmma, ymma, zmma, lam, xsi, eta, mu, zet, s, low, upp] = ...
    mmasub(m, n, iter, xval, xmin, xmax, xold1, xold2, ...
    f0val, df0dx, fval, dfdx, low, upp, a0, a, c, d);
```

2.6 Topology optimization problems

By taking different boundary conditions and making some changes in the code give rise to different topology optimization problems such as half of the "MBB beam", short cantilever beam and cantilever beam with a fixed circular hole. For all three optimization problems, the vertical unit force is shown in the Figure (2.1). Supports are implemented by eliminating fixed degrees of freedom from the linear equation which are obtained by finite element method. Both nodes and elements are numbered column wise from left to right. For each iteration in the topology optimization loop, the code generates a picture of the current density distribution depending on the boundary conditions.

In MMA the move limit parameter is "0.2" for all problems. By taking move limit parameter "1.0" one gets Svanberg's original MMA, the only purpose to choose move limit parameter "0.2" is to get a more stable solution process. In order to get a better convergent solution for both optimality techniques "0.01" termination criterion is used. It is observed that when these topology optimization problems are solved with MMA and OC, the optimality technique MMA took less iterations as compared to OC but CPU-time increased per iteration.

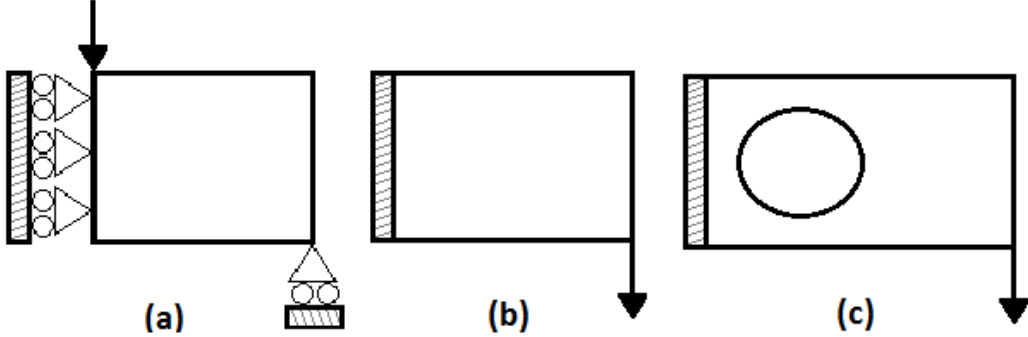


Figure 2.1. (a) Half MBB beam, (b) Short cantilever beam, (c) Cantilever beam with a fixed hole.

2.6.1 Half MBB beam

The simply-supported Messerschmitt-Bölkow-Blohm (MBB) Beam: half design domain with symmetry boundary conditions shown in the Figure (2.1(a)) is optimized for minimum compliance. Due to the overall symmetry, the computational model represents one half of the physical domain. The following boundary condition leads to the half MBB Beam problem.

$$\begin{aligned} F(2,1) &= -1; \\ \text{fixeddofs} &= \text{union}([1 : 2 : 2 * (\text{nely} + 1)], [2 * (\text{nelx} + 1) * (\text{nely} + 1)]); \end{aligned} \quad (2.7)$$

The load is applied vertically in the upper left corner and there is symmetric boundary condition along the left edge and the structure is supported horizontally in the lower right corner.

Input line is: $(\text{nelx}, \text{nely}, \text{volfrac}, \text{penal}, \text{rmin}) = (60, 20, 0.5, 3.0, 1.5)$,

where nelx and nely are the number of elements in the horizontal and vertical directions, respectively, volfrac is the volume fraction, penal is the penalization power, rmin is the filter size (divided by element size) [19]. The topology optimization problem for half MBB beam solved with OC and MMA is shown in Figure (2.2). The filtered optimal topology of OC is obtained after 94 iterations with objective value 203.3061 whereas in case of MMA it takes 70 iterations with objective value 203.2381.

2.6. TOPOLOGY OPTIMIZATION PROBLEMS

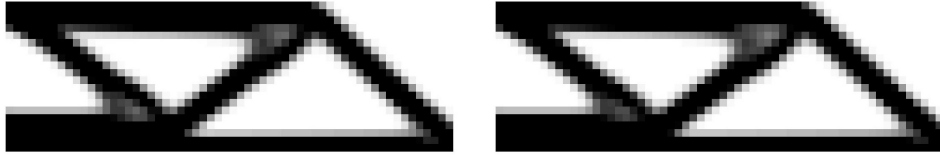


Figure 2.2. Half MBB beam solved by OC on left and MMA on right

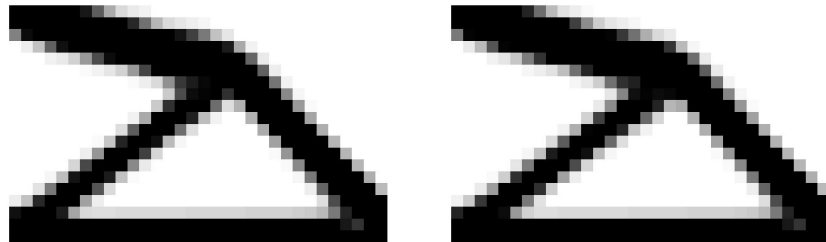


Figure 2.3. Short cantilever beam solved by OC on left and MMA on right

2.6.2 Short cantilever beam

For short cantilever beam optimization problem as shown in the Figure (2.1(b)), the boundary condition is:

$$\begin{aligned} F(2 * (\text{nelx} + 1) * (\text{nely} + 1), 1) &= -1; \\ \text{fixeddofs} &= [1 : 2 * (\text{nely} + 1)]; \end{aligned} \quad (2.8)$$

where the command $F(2, 1) = -1$ is a vertical unit force in the lower right corner and `fixeddofs` are the fixed degrees of freedom. The Figure (2.3) shows the comparison of cantilevered beam with those based on the OC method on the left and MMA on the right for 40% volume. The results are based on the filtering radius of $r = 1.2$. In case of OC, 71 iterations are used to optimize the problem having objective value 57.3492 whereas in case of MMA 50 iterations are needed to have an optimal solution of objective value 57.2722.

Input line: (`nelx` , `nely`, `volfrac`, `penal`, `rmin`) = (32, 20, 0.4, 3.0, 1.2).



Figure 2.4. Cantilever beam with a fixed hole solved by OC on left and MMA on right

2.6.3 Cantilever beam with a fixed hole

In the optimal topology for a cantilevered beam with a fixed circular hole as shown in the Figure (2.1(c)) some of the elements may be required to take the minimum density value. The hole is modeled using **passive** elements with a circle of radius $\text{nely}/3.$ and center $(\text{nely}/2., \text{nelx}/3.).$ The zeros at elements free to change and ones at elements fixed to be zero. The load is applied vertically in the lower right corner.

The added lines are:

```

x(find(passive)) = 0.001;
for ely = 1 : nely
    for elx = 1 : nelx
        if  $\sqrt{(ely - \text{nely}/2.)^2 + (elx - \text{nelx}/3.)^2} < \text{nely}/3.$ 
            passive(ely, elx) = 1;
            x(ely, elx) = 0.001;
        else
            passive(ely, elx) = 0;
        end
    end
end

```

Figure (2.4) shows the comparison of OC on the left with MMA on the right. In case of OC the total number of iterations are 34 having objective value 52.1080 whereas in case of MMA it takes 22 iterations with objective value 53.0281. The resulting structure obtained with the input:

$$(\text{nelx}, \text{nely}, \text{volfrac}, \text{penal}, \text{rmin}) = (45, 30, 0.5, 3.0, 1.5).$$

2.7. CONTINUATION PROCEDURE

By solving the three topology optimization problems, it is observed that the optimal solution by both methods are almost the same but OC works better than MMA. This is because, OC is developed for these kind of problems where only single constraint is involved and secondly the filter which is used here do not calculate the derivatives exactly "correct". So may be MMA is more sensitive to such kind of filter than that of OC.

2.7 Continuation procedure

The purpose to solve topology optimization problem by using continuation procedure is to show the effect of penalization parameter by taking its value $p = 1, 2$ and 3 . The continuation procedure is to start the problem by taking penalization parameter $p = 1$. Solve the problem to get the optimal solution. Let this optimal solution be the starting point of the problem for penalization parameter $p = 2$. Then solve the problem again and let the optimal solution be the starting point of the problem for penalization parameter $p = 3$. Solve this problem to get the final result. Figure (2.5) to (2.7) schematically shows the evolution of the topology during optimization process with MMA.

2.8 Results and Discussion

All three topology optimization problems which are stated in section (2.6) are solved by continuation procedure using method of moving asymptotes based optimizer.

2.8.1 MBB beam

A simply-supported Half MBB beam (2.7) with (nelx , nely , volfrac , penal , rmin) = (60, 20, 0.5, 3.0, 1.5), is optimized by continuation procedure using MMA is shown in the Figure (2.5). For $p = 1$ the number of iterations are 6 and the objective value is 164.7850, for $p = 2$ it takes 33 iterations to give optimal solution having objective value 199.3333. Finally, for $p = 3$ the number of iterations are 8 with objective value 203.1884.

2.8.2 Short cantilever beam

Short cantilever beam (2.8) is optimized with the same input as used in (2.6.2). For $p = 1$ the number of iterations are 6 and the objective value is 45.5047, for $p = 2$ it

CHAPTER 2. TOPOLOGY OPTIMIZATION PROBLEM FOR COMPLIANCE
MINIMIZATION

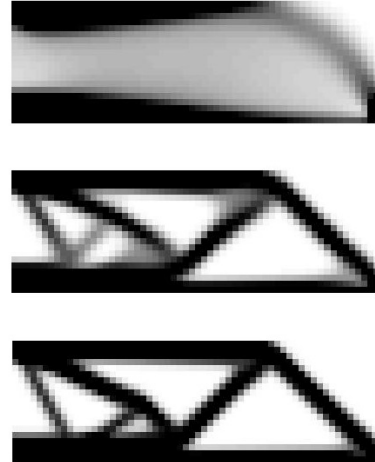


Figure 2.5. Half MBB beam solved by continuation procedure with MMA

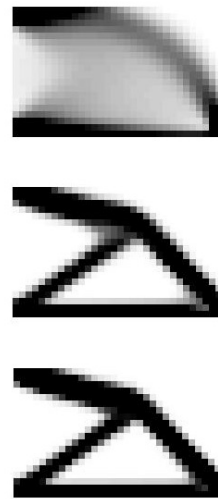


Figure 2.6. Short cantilever beam solved by continuation procedure with MMA

takes 19 iterations to give optimal solution having objective value 55.9763. Finally, for $p = 3$ the number of iterations are 12 with objective value 57.1348 shown in the Figure (2.6).

2.8. RESULTS AND DISCUSSION



Figure 2.7. Cantilever beam with a fixed hole solved by continuation procedure with MMA

2.8.3 Cantilever beam with a fixed hole

Cantilever beam with a fixed circular hole is optimized by continuation procedure with those based on the MMA for a volume fraction of 50%. The results are based on the filtering radius of $r = 1.5$ (see 2.6.3). For $p = 1$ the number of iterations are 6 and the objective value is 49.6115, for $p = 2$ it takes 13 iterations to give optimal solution having objective value 51.5592. Finally, for $p = 3$ the number of iterations are 19 with objective value 53.0281 shown in the Figure (2.7).

By solving the three topology optimization problems, it is observed that in order to obtain true 0-1 (i.e. white and black) design the penalization parameter $p = 3$ is required. For this choice of p the intermediate densities are penalized as it is clearly seen in all the three Figures (2.5) to (2.7).

Chapter 3

Comparison of SIMP model and alternative model

3.1 Introduction

In this chapter, An alternative interpolation scheme developed by Stolpe M and Svanberg K [21]; for minimum compliance topology optimization is compared with SIMP model. The implemented algorithm for both model is method of moving asymptotes. All three topology optimization problems of previous chapter half MBB beam, short cantilever beam and cantilever beam with a fixed hole are discussed here.

3.2 SIMP model

In SIMP (Solid Isotropic Material with Penalization) approach, a nonlinear interpolation model for the material properties in terms of selection field is used. For each element, material properties are assumed constant and used to discretize the design domain. This interpolation is essentially a power law (3.1) that interpolates the Young's modulus of the material to the scalar selection field, where the binary constraints are relaxed and intermediate values are penalized by replacing x_j by x_j^p for some given parameter p varies between [1, 3], in general, in the equilibrium equations. The intermediate values give very little stiffness in comparison to the amount of material used. The penalized compliance $c_p(\mathbf{x})$ in SIMP does not necessarily become a concave function, no matter how large p is chosen [22]. For the

two-material problem the SIMP interpolation model can be expressed as:

$$E_p(x_j) = E_0 + x_j^p \Delta E \quad (3.1)$$

satisfies $E_p(0) = E_0, \quad E_p(1) = E_1.$

where $\Delta E = E_1 - E_0$, while E_0 and E_1 are the Young moduli and it is assumed that $E_1 > E_0 > 0$. For a given parameter $p \geq 1$, the SIMP problem is defined as:

$$\min_{\mathbf{x} \in X_p} \quad c_p(\mathbf{x}) = \mathbf{f}^T \mathbf{K}_p(\mathbf{x})^{-1} \mathbf{f},$$

where $\mathbf{K}_p(\mathbf{x}) = \sum_{j=1}^n E_p(x_j) \mathbf{K}_j.$

3.3 Alternate model

Also in the alternate material model, the approach is to relax the zero-one constraints and model the material properties by a law which gives non-integer solutions very little stiffness in comparison to the amount of material used. It was proved in [21]; that in this model the penalized compliance $c_q(\mathbf{x})$ becomes a concave function for sufficiently large q . For the two-material problem the alternative interpolation model can be expressed as:

$$E_q(x_j) = E_0 + x_j / (1 + q(1 - x_j)) \Delta E. \quad (3.2)$$

$$\text{satisfies } E_q(0) = E_0, \quad E_q(1) = E_1. \quad (3.3)$$

where q is a penalty parameter, $c_q(\mathbf{x})$ is convex for $q = 0$ and concave for $q \geq \Delta E/E_0$, see [21]. The penalized problem is defined as:

$$\min_{\mathbf{x} \in X_p} \quad c_q(\mathbf{x}) = \mathbf{f}^T \mathbf{K}_q(\mathbf{x})^{-1} \mathbf{f},$$

where $\mathbf{K}_q(\mathbf{x}) = \sum_{j=1}^n E_q(x_j) \mathbf{K}_j.$

Let $E_q(x_j)$ denote the alternative interpolation model defined in (3.3) for a parameter $q \geq 0$, i.e.,

$$E_q(x_j) = E_0 + \frac{x_j}{(1 + q(1 - x_j))} \Delta E. \quad (3.4)$$

3.4. RESULTS AND DISCUSSION

Differentiating $E_q(x_j)$ gives:

$$E'_q(x_j) = \frac{\Delta E(1+q)}{[1+q(1-x_j)]^2} > 0 \quad (3.5)$$

and

$$E''_q(x_j) = \frac{2q\Delta E(1+q)}{[1+q(1-x_j)]^3} \geq 0. \quad (3.6)$$

One of the major differences between the SIMP model and the alternative model is the behavior of the derivative of the material model at $x_j = 0$, [21]. Evaluating the derivative of the alternative model and SIMP model at zero and one and comparing them shows that $E'_p(0)$ is discontinuous in SIMP model in the parameter p whereas $E'_q(0)$ is continuous in the parameter q in alternative model.

$$E'_q(0) = \frac{1}{1+q} \Delta E > 0 \text{ and } E'_q(1) = (1+q)\Delta E. \quad (3.7)$$

$$E'_p(0) = \begin{cases} \Delta E & \text{if } p = 1, \\ 0 & \text{if } p > 1, \end{cases} \quad \text{and}$$

$$E'_p(1) = p \Delta E. \quad (3.8)$$

3.4 Results and Discussion

The topology optimization problems which discussed in chapter 2 solved again. Here considered four different scenarios, these problems are solved for SIMP model and also with alternate model objective function. And then considered alternate model and also solved with SIMP model objective function. The optimization technique used is method of moving asymptotes for all the possible cases.

3.4.1 MBB beam

Topology optimization problem of half MBB beam is solved for alternate model with penalized compliance $q = 9.0$, and in case of SIMP model penalization parameter is $p = 3.0$. The results obtained by both models is shown in the Table (3.1).

CHAPTER 3. COMPARISON OF SIMP MODEL AND ALTERNATIVE MODEL

Model	SIMP objective function	Alternate objective function
SIMP	203.2381	220.8406
Alternate	194.0418	205.9436

Table 3.1. Half MBB beam with alternate model and SIMP model

Model	SIMP objective function	Alternate objective function
SIMP	57.2722	61.0940
Alternate	53.8452	61.9126

Table 3.2. Short cantilever beam with alternate model and SIMP model

Model	SIMP objective function	Alternate objective function
SIMP	53.0281	56.2405
Alternate	51.3723	53.0245

Table 3.3. Cantilever beam with a fixed hole with alternate model and SIMP model

3.4.2 Short cantilever beam

When short cantilever beam is solved for alternate model with penalized compliance $q = 9.0$ and penalization parameter is $p = 3.0$ in case of SIMP model, the results obtained are shown in Table (3.2).

3.4.3 Cantilever beam with a fixed hole

Topology optimization problem of cantilever beam with a fixed hole is solved for alternate model with penalized compliance $q = 9.0$ and in case of SIMP model penalization parameter is $p = 3.0$. The results obtained by both models is shown in the Table (3.3).

It is observed that in the three studied topology optimization problems, the obtained structures are very similar for both models in all cases. The optimal solution is slightly better for alternate model with SIMP model objective function for all three problems.

3.4. RESULTS AND DISCUSSION

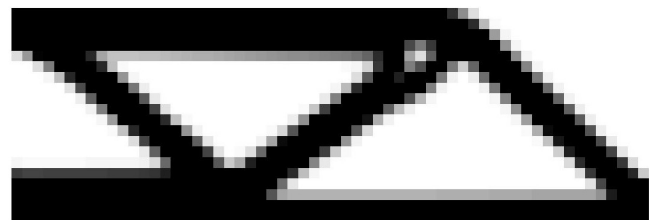


Figure 3.1. Half MBB beam solved with alternate model

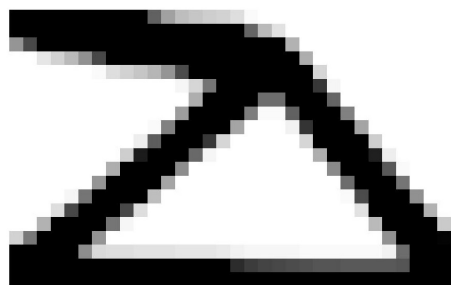


Figure 3.2. Short cantilever beam solved with alternate model

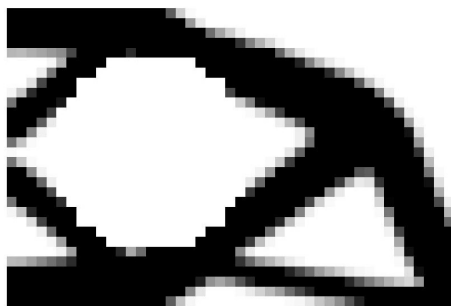


Figure 3.3. Cantilever beam with a fixed hole solved with alternate model

Chapter 4

Four node square elements, nine node square elements and six node hexagonal elements

4.1 Introduction

The purpose of this chapter is to compare three different types of finite elements for topology optimization. The reason of using nine node square elements and six node hexagonal elements is because of the checkerboard pattern that appeared in square four node elements when solved without filter. It is showed by Diaz AR and Sigmund O [6]; that the checkerboard pattern occurs because it has a numerically induced (artificially) high stiffness compared with a material with uniform material distribution. So possible ways to prevent checkerboard is to use some filter technique or to use higher order elements. This, however, increases the computational time.

4.2 Finite elements used

In this part of the report, the finite element equations for the stress analysis subjected to some external loads and support is solved. As discussed earlier, for simplicity all numerical examples in this thesis are two-dimensional. Therefore, the element used for the structural problems where the loading and the deformation occur within the plane is called *a 2D solid element*. In our case 2D solid element is square in shape for four node with bilinear shape functions and nine node with quadratic shape functions therefore the edges are straight as shown in Figure (4.4)

CHAPTER 4. FOUR NODE SQUARE ELEMENTS, NINE NODE SQUARE ELEMENTS AND SIX NODE HEXAGONAL ELEMENTS

(a)). In case of six node it is hexagonal element with Wachspress shape functions. Order of the shape functions are used to determined the order of the 2D element. The equation system for 2D have following three steps:

1. Construction of *shape functions* matrix \mathbf{N} that satisfies Delta function property and Partition of unity (Appendix A.3.1).
2. Formulation of the *strain matrix* \mathbf{B} .
3. Calculation of stiffness matrix \mathbf{k}_e by using shape function \mathbf{N} and strain matrix \mathbf{B} in Eq. (A.4).

4.3 Four node square element

For square four node element the domain is discretized into a number of *square elements* with four nodes and four straight edges. The nodes are numbered in counter-clockwise direction in each element as 1, 2, 3 and 4. The number of possible directions that displacements or forces at a node can exist in is termed a *degree of freedom* (DOF). The degrees of freedom (DOF) for each node is two, therefore the total number of DOF is eight for square four node element.

A local *natural coordinate system* (ξ, η) is defined with its origin located at the center of the element is shown in the Figure (4.1). The local node numbering is also shown in it. As discussed above, the very first task is to construct shape functions and that can be found in Appendix (B.1) for square four node. The shape functions satisfied the delta function property and partition of unity. The next step is to derive strain matrix required for computing the stiffness matrix of the element. The strain matrix is obtained with the use of shape function as: $\mathbf{B} = \mathbf{LN}$, where \mathbf{L} is differential operator (see Appendix A.4). Once the shape function and strain matrix is obtained, the element stiffness matrix \mathbf{k}_e is obtained with the use of equation (A.4).

4.4 Nine node square element

In case of square nine node element, the domain is discretized into a number of *square elements* with nine nodes and four straight edges. The nodes are numbered in counter-clockwise direction in each element as 1, 2, 3 and 4 on the corner of the square element. 5, 6, 7 and 8 are in the middle of the edges whereas 9 is in the

4.5. SIX NODE HEXAGONAL ELEMENT

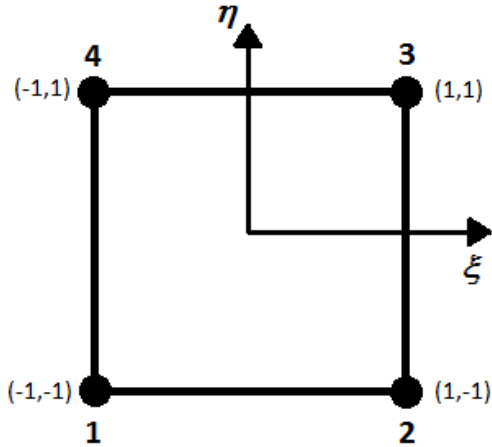


Figure 4.1. The finite element four node in local coordinates (ξ, η) . The local node numbering is also shown.

center of the element as shown in the Figure (4.2). The degrees of freedom (DOF) for each node is two, therefore the total number of DOF are 18 for each square nine node element.

Similarly, as in case of square four node a local *natural coordinate system* (ξ, η) is defined for square nine node with its origin located at the center of the element as shown in Figure (4.2). The local node numbering is also shown here. The shape functions constructed for square nine node can be found in Appendix (B.2). These shape functions also satisfies the delta function property and partition of unity. The strain matrix is obtained with the use of shape functions. After getting shape functions and strain matrix, the element stiffness matrix \mathbf{k}_e is calculated.

4.5 Six node hexagonal element

Six node hexagonal element (honeycomb) is one of the feasible alternative to avoid checkerboard pattern with Wachspress shape functions [27]. In our case mesh is uniform, so any two hexagonal elements that share an edge have two common vertices as shown in Figure (4.3). Thus there are two-node connections in hexagonal element which means that the two elements are either connected by two nodes or not connected at all. So it excludes the unwanted formation of checkerboard without

CHAPTER 4. FOUR NODE SQUARE ELEMENTS, NINE NODE SQUARE ELEMENTS AND SIX NODE HEXAGONAL ELEMENTS

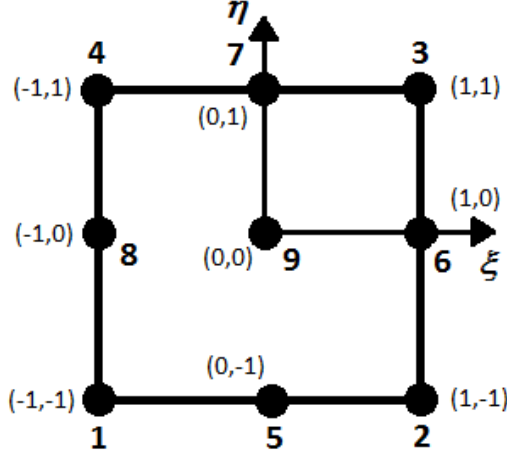


Figure 4.2. The finite element nine node in local coordinates (ξ, η) . The local node numbering is also shown.

imposing any further restrictions (like filtration). The other feature of having uniform mesh is that there are three edge-based symmetry lines per element as shown in Figure (4.4 (b)). This aspect allows to suffer less from directional constraint and allows for a more flexible arrangement of the final layout in the optimization process.

In this thesis Wachspress shape functions are used for hexagonal element (see Appendix B.3). These shape functions are bounded, non-negative and form a partition of unity. And also satisfy delta function property (A.3.1). For numerical integration, fully symmetric quadrature rules are developed for regions with regular hexagonal symmetry [26]. The list of quadrature points for various values of j can be found in Appendix (C.2).

4.6 Results and Discussion

The topology optimization problem for compliance minimization is solved for four node square elements with filter and without filter, nine node square elements and six node hexagonal elements with method of moving asymptotes based optimizer. In MMA move limit parameter "0.2" is used for all the cases to get a slightly more stable solution process in comparison with move limit "1.0". For all the three types of finite elements 40% volume and 50% volume taken into consideration, the penalization parameter, p , is 3 and the number of elements used to discretize the

4.6. RESULTS AND DISCUSSION

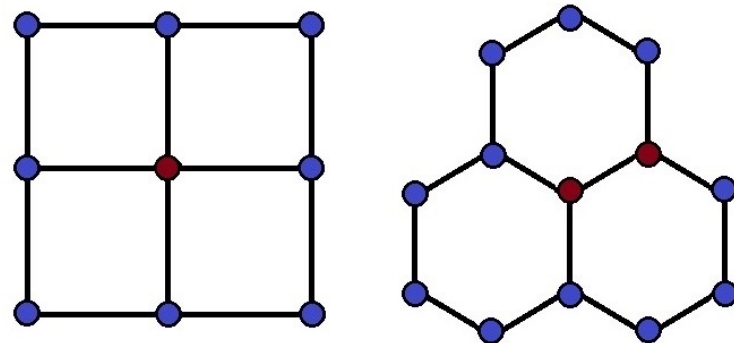


Figure 4.3. Square element mesh can display one node-connection while in a hexagonal mesh two connected elements always share two nodes through as edge connection

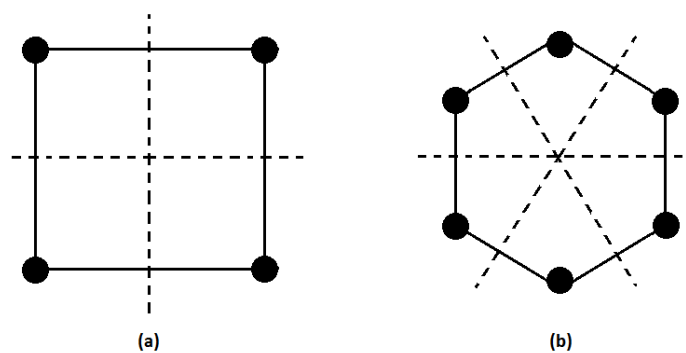


Figure 4.4. The square element has two edges-based-symmetry lines whereas hexagonal element has three edge-based symmetry lines

CHAPTER 4. FOUR NODE SQUARE ELEMENTS, NINE NODE SQUARE ELEMENTS AND SIX NODE HEXAGONAL ELEMENTS

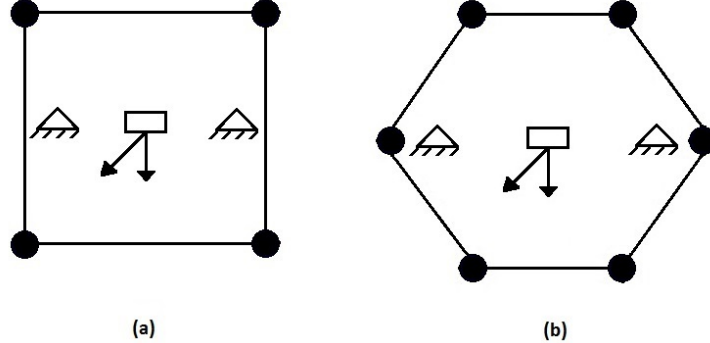


Figure 4.5. Design Domain, loads and support for square element (a) and hexagonal element (b)

design domain, N , is 60×60 and 80×80 . The structure is supported in the middle of the left and right sides not on the boundary of the structure but a little on the inside element of the structure which are fixed in both vertical and horizontal directions. The load is applied in the central element as shown in the Figure (4.5).

For four node square elements and nine node square elements when we say 40% volume and 50% volume it means 26% volume and 32.5% volume, respectively. The reason is that 40% of the hexagonal design space, in for example Figure (4.9), corresponds to 26% of the square design space, in for example Figure (4.6) so that the area covered by the square finite element is comparable with the area covered by hexagonal finite element.

For a fair comparison of the three finite elements, the topology optimization problem is also solved for 100% volume for hexagonal finite element and 65% volume for square finite elements (with the same reason as mentioned above) to get a black solution. Then taking the ratio of the compliance of obtained optimal solution for both 40% and 50% volume by the compliance of obtained black solution for all finite elements. This calculation is also shown in the Tables (4.1), (4.2), (4.3) and (4.4).

Another topology optimization problem is obtained by tilting the load $(0, -1)$ in the center of the element to $(-1/2, -1)$ while all the other parameters remains the same can be seen in Figure (4.5). The problem is solved for all the three finite

4.6. RESULTS AND DISCUSSION

Finite Elements	Filter	Number of iterations	Optimal solution / Black solution
Four node	No	34	2.3512
	Yes	76	2.3000
Nine node	No	39	2.2159
Six node	No	35	2.1049

Table 4.1. Volume 40%, Number of elements 60×60

elements with 40% volume and 50% volume and the number of elements used to discretize the design domain is 80×80 .

4.6.1 40% Volume

Case I - 60×60

In Case I, the number elements used to discretize the design domain for 40% volume is 60×60 . The topology optimization problem is solved with all the three finite elements are shown in Figures (4.6, 4.7, 4.8, 4.9). The results obtained by solving topology optimization problem is shown in Table (4.1).

CHAPTER 4. FOUR NODE SQUARE ELEMENTS, NINE NODE SQUARE ELEMENTS AND SIX NODE HEXAGONAL ELEMENTS

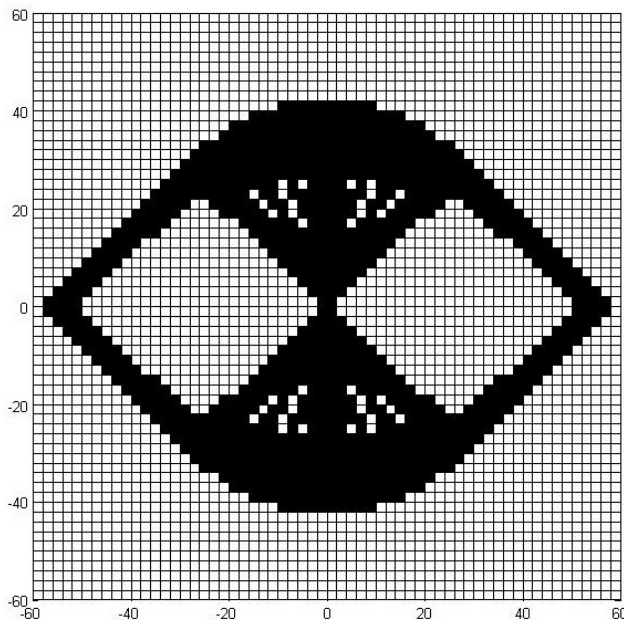


Figure 4.6. Four node square elements without filter; Volume 40%, $N = 60 \times 60$

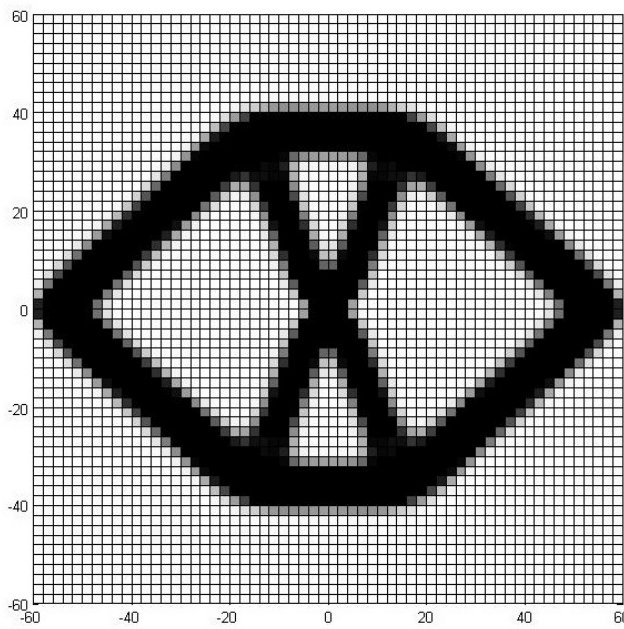


Figure 4.7. Four node square elements with filter; Volume 40%, $N = 60 \times 60$

4.6. RESULTS AND DISCUSSION

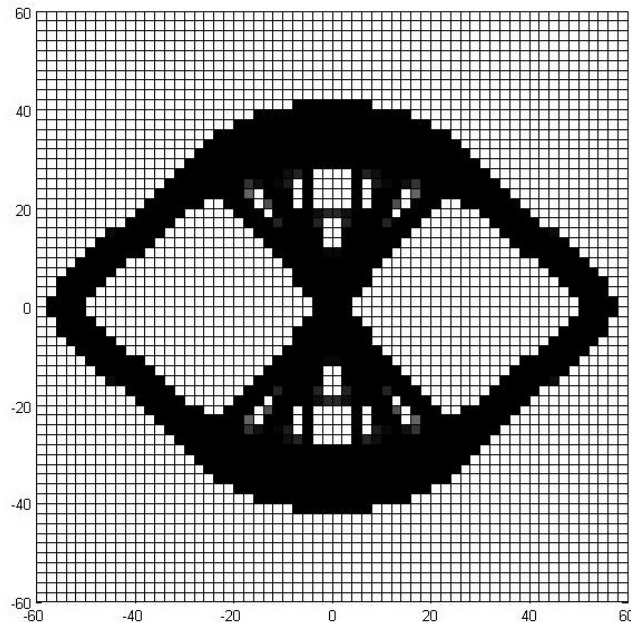


Figure 4.8. Nine node square elements; Volume 40%, $N = 60 \times 60$

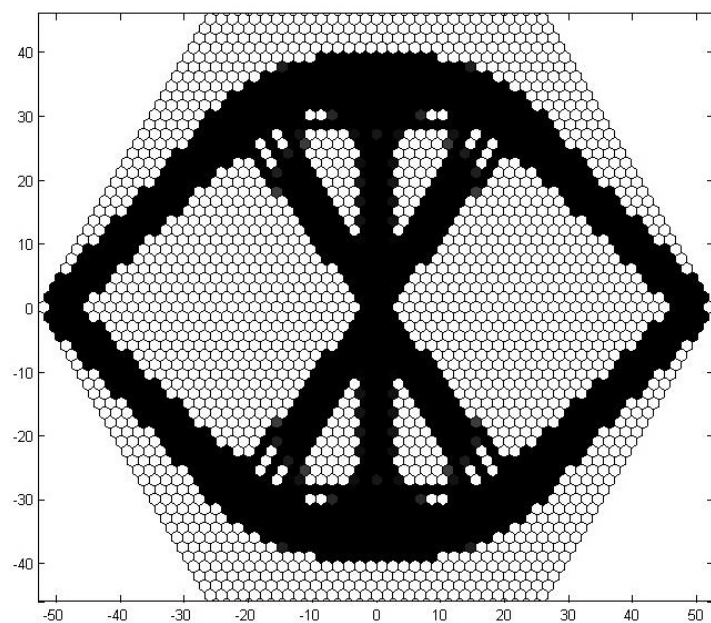


Figure 4.9. Six node hexagonal elements; Volume 40%, $N = 60 \times 60$

CHAPTER 4. FOUR NODE SQUARE ELEMENTS, NINE NODE SQUARE ELEMENTS AND SIX NODE HEXAGONAL ELEMENTS

Finite Elements	Filter	Number of iterations	Optimal solution / Black solution
Four node	No	29	2.2544
	Yes	72	2.2018
Nine node	No	44	2.1618
Six node	No	32	1.9734

Table 4.2. Volume 40%, Number of elements 80×80

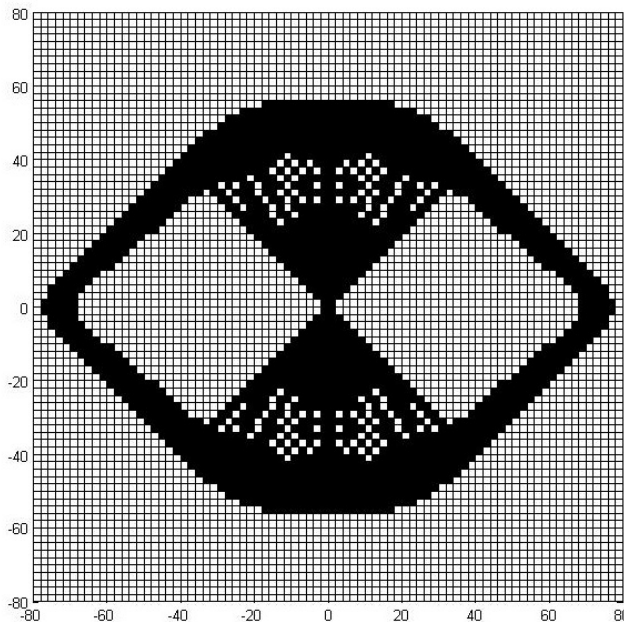


Figure 4.10. Four node square element without filter; Volume 40%, $N = 80 \times 80$

Case II - 80×80

In Case II, the number of elements used to discretize the design domain is 80×80 while volume remain the same. By solving the topology optimization problem for four node square elements (with and without filter), nine node square elements and six node hexagonal elements the results obtained are shown in Table (4.2). The picture generated while solving the three finite elements are shown in Figures (4.10, 4.11, 4.12, 4.13).

4.6. RESULTS AND DISCUSSION

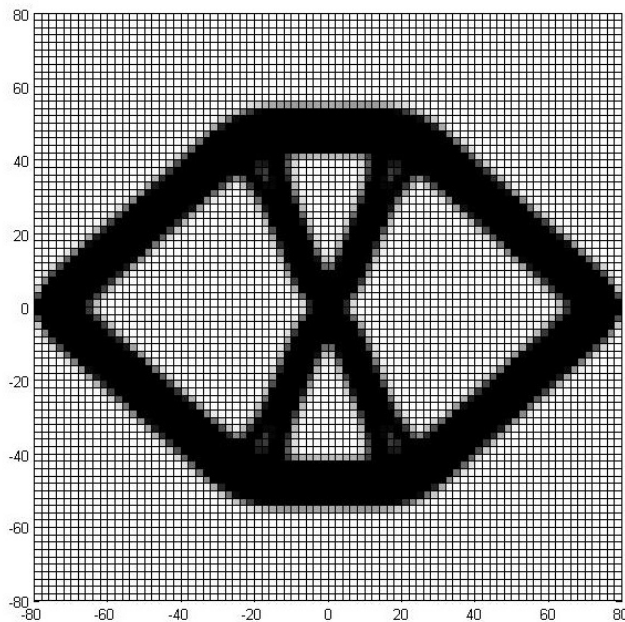


Figure 4.11. Four node square element with filter; Volume 40%, $N = 80 \times 80$

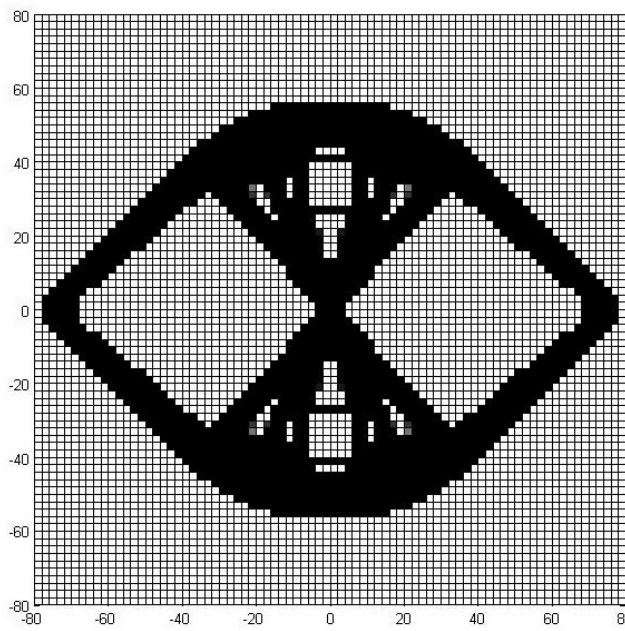


Figure 4.12. Nine node square element; Volume 40%, $N = 80 \times 80$

CHAPTER 4. FOUR NODE SQUARE ELEMENTS, NINE NODE SQUARE ELEMENTS AND SIX NODE HEXAGONAL ELEMENTS

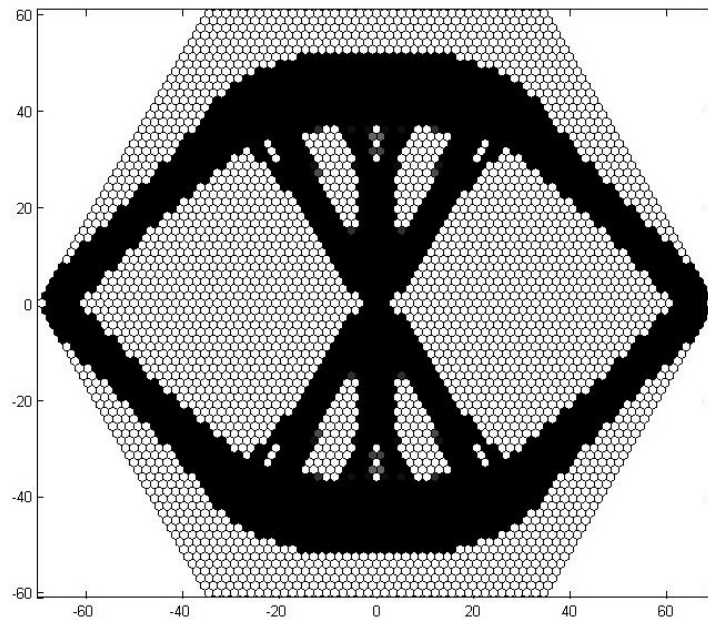


Figure 4.13. Six node hexagonal element; Volume 40%, $N = 80 \times 80$

Finite Elements	Filter	Number of iterations	Optimal solution / Black solution
Four node	No	41	1.8158
	Yes	52	1.8103
Nine node	No	32	1.7230
Six node	No	32	1.6517

Table 4.3. Volume 50%, Number of elements 60×60

4.6.2 50% Volume

Case I - 60×60

In Case I, the number elements used to discretize the design domain for 50% volume is 60×60 . The topology optimization problem is solved with all the three finite elements are shown in Figures (4.14, 4.15, 4.16, 4.17). The results obtained by solving topology optimization problem is shown in Table (4.3).

4.6. RESULTS AND DISCUSSION

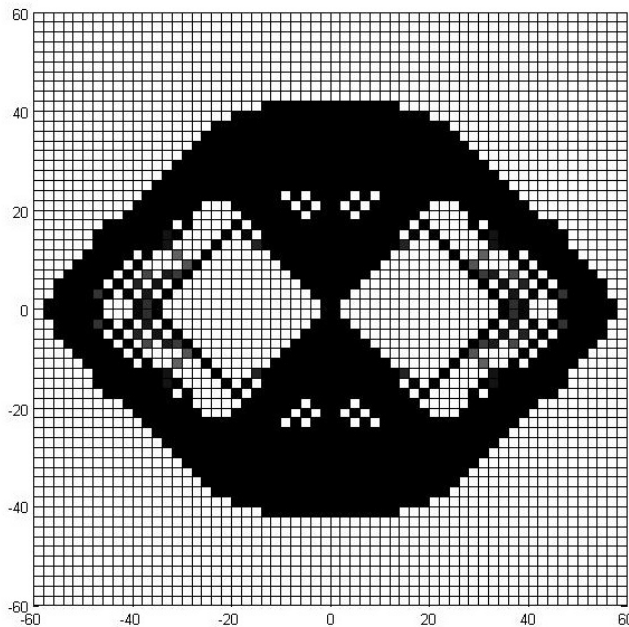


Figure 4.14. Four node square elements without filter; Volume 50%, $N = 60 \times 60$

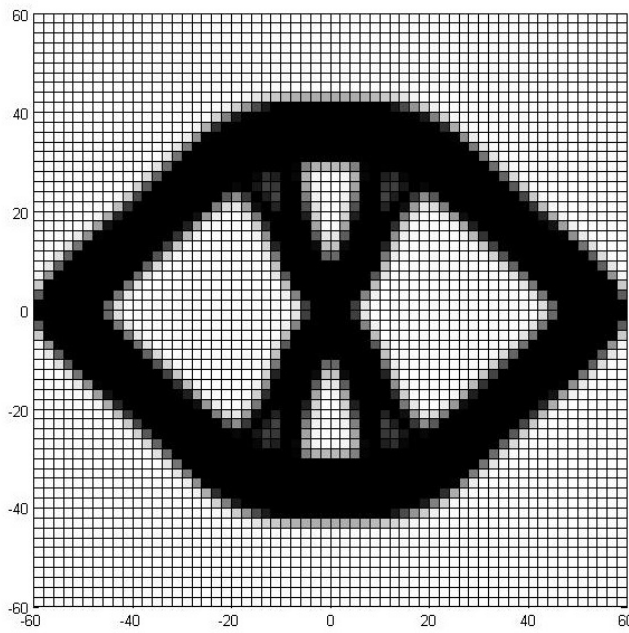


Figure 4.15. Four node square elements with filter; Volume 50%, $N = 60 \times 60$

CHAPTER 4. FOUR NODE SQUARE ELEMENTS, NINE NODE SQUARE ELEMENTS AND SIX NODE HEXAGONAL ELEMENTS

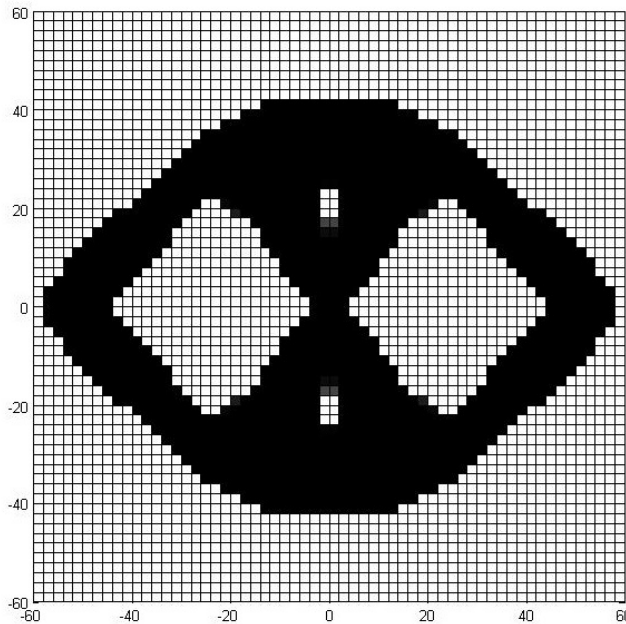


Figure 4.16. Nine node square elements; Volume 50%, $N = 60 \times 60$

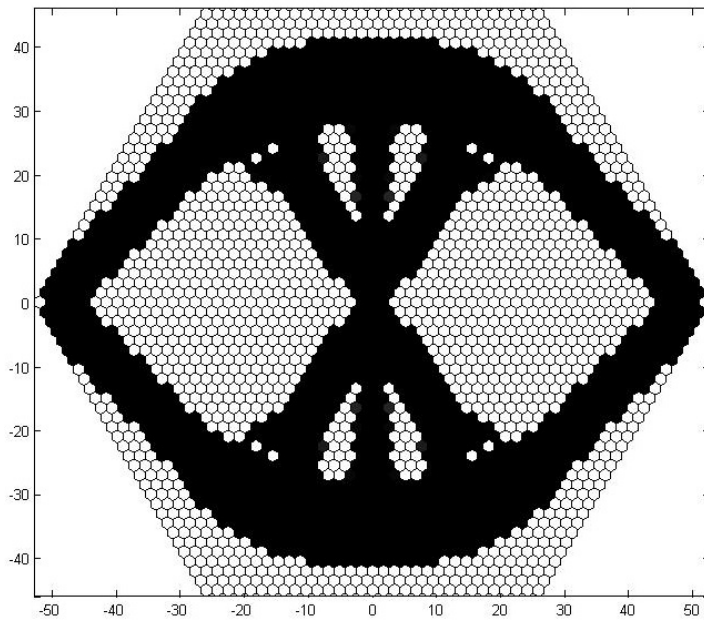


Figure 4.17. Six node hexagonal elements; Volume 50%, $N = 60 \times 60$

4.6. RESULTS AND DISCUSSION

Finite Elements	Filter	Number of iterations	Optimal solution / Black solution
Four node	No	28	1.7791
	Yes	156	1.7661
Nine node	No	42	1.7034
Six node	No	39	1.5844

Table 4.4. Volume 50%, Number of elements 80×80

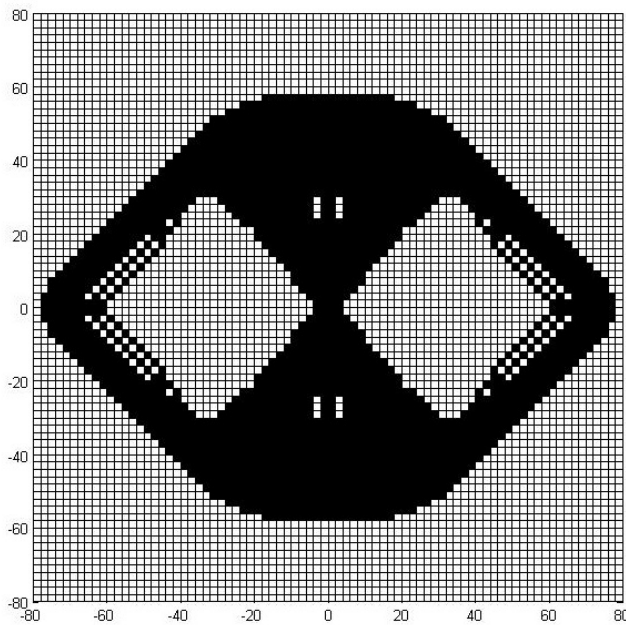


Figure 4.18. Four node square elements without filter; Volume 50%, $N = 80 \times 80$

Case II - 80×80

In Case II, the volume remain the same but number of elements increased to 80×80 to discretize the design domain. The results obtained by solving the topology optimization problem with four node square elements (with and without filter), nine node square elements and six node hexagonal elements are shown in Table (4.4). The picture generated in this case are shown in Figures (4.18, 4.19, 4.20, 4.21).

As discussed before, two elements in a hexagonal mesh either share one edge or not connected at all. Therefore, the geometric nature of hexagon Wachspress

CHAPTER 4. FOUR NODE SQUARE ELEMENTS, NINE NODE SQUARE ELEMENTS AND SIX NODE HEXAGONAL ELEMENTS

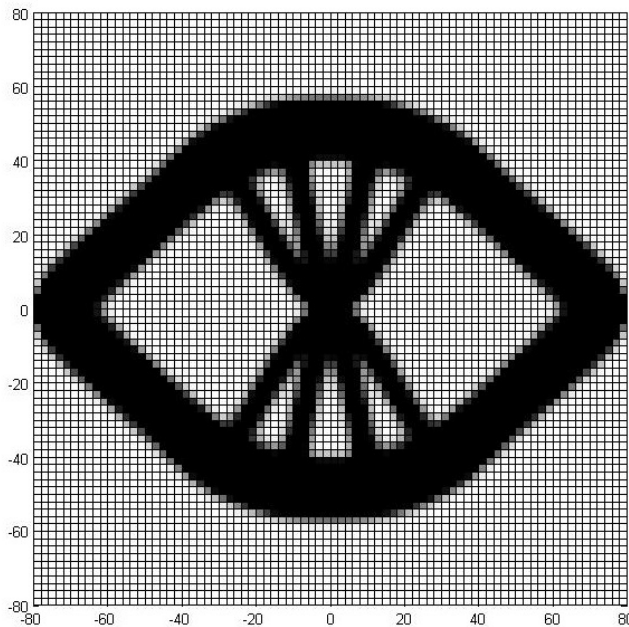


Figure 4.19. Four node square elements with filter; Volume 50%, $N = 80 \times 80$

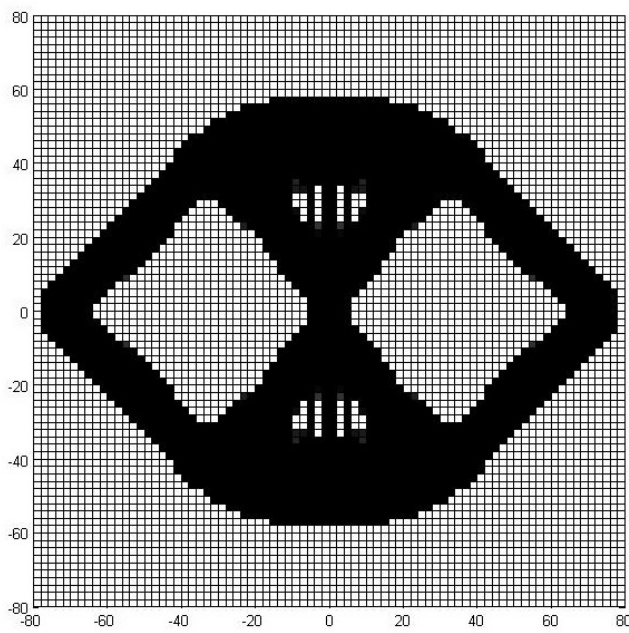


Figure 4.20. Nine node square elements; Volume 50%, $N = 80 \times 80$

4.6. RESULTS AND DISCUSSION

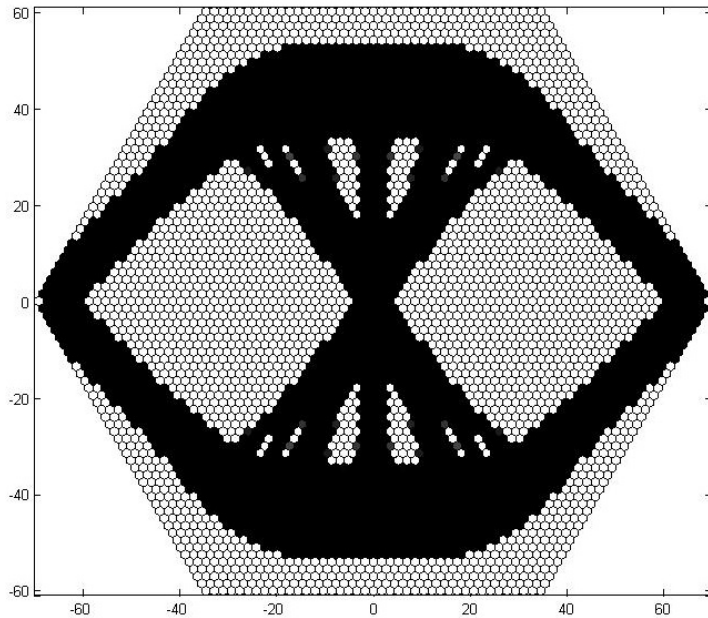


Figure 4.21. Six node hexagonal elements; Volume 50%, $N = 80 \times 80$

element can eliminate the severe error in the density representation that is observed with four node square elements in the form of checkerboard when solved without filter. Although the more accurate approximation of the displacement field may resolve the checkerboard problem for nine node square elements, but they may also suffer from one node hinges. With hexagonal mesh undesired small scale patterns may also be possible but still Wachspress element are more stable element for topology optimization.

As it is observed in all the cases that for four node square element checkerboard pattern appeared when it is solved without filter. Checkerboard pattern is avoided by using filtration. For nine node square elements and six nodes hexagonal elements no filtration is required and the resulting solid-void solution satisfies the imposed volume but in both cases a number of holes are observed. By taking the ratio of the compliance optimal solution to the compliance of black solution it is observed that six node hexagonal elements gives the lowest value in all the scenarios, so one can say that it gives a better optimal solution. Nine node square elements are better than four node square element with filter.

CHAPTER 4. FOUR NODE SQUARE ELEMENTS, NINE NODE SQUARE ELEMENTS AND SIX NODE HEXAGONAL ELEMENTS

To solve the topology optimization problem we used a machine with MATLAB version 7.10.0.499 (R2010a), 64-bit. The CPU is a Intel Core i3 M330 @ 2.13 GHz with 2.00 GB of 2.13 GHz RAM and observed that the nine node square elements are very expensive in computation as at least 200 minutes was taken by machine. For six node hexagonal elements 180 minutes, for four node square elements with filter 150 minutes and for four node square elements without filter 120 minutes.

We also solved the topology optimization problem by fixing the supports only in vertical direction and are free to move horizontally, while the load is applied vertically and fixed horizontally. All the three finite elements are solved for 40% and 50% volume, by taking penalization parameter $p = 3$, number of elements used to discretize the design domain are 60×60 and 80×80 . The results are almost the same as calculated previously.

4.7 Another load condition

In order to obtained another optimization problem the load which is at $(0, -1)$ in the center of the element changed by tilting it to $(-1/2, -1)$ while the supports remains the same. All the three finite elements are solved for 40% volume and 50% volume, penalization parameter p is 3, the number of elements used to discretize the design domain is 80×80 .

4.7.1 40% Volume - 80×80

In Case of 40% volume the topology optimization problem is solved for four node square elements (with and without filter), nine node square elements and six node hexagonal elements and the results obtained are shown in Table (4.5). The picture generated for all the cases can be seen in Figures (4.22, 4.23, 4.24, 4.25).

4.7. ANOTHER LOAD CONDITION

Finite Elements	Filter	Number of iterations	Optimal solution / Black solution
Four node	No	52	2.1879
	Yes	131	2.2489
Nine node	No	52	2.1696
Six node	No	39	2.0777

Table 4.5. Volume 40%, Number of elements 80×80

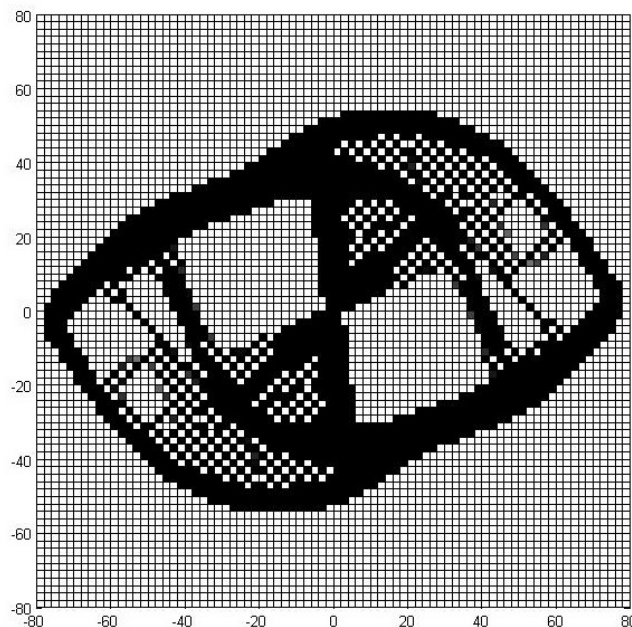


Figure 4.22. Four node square elements without filter; Volume 40%, $N = 80 \times 80$

CHAPTER 4. FOUR NODE SQUARE ELEMENTS, NINE NODE SQUARE ELEMENTS AND SIX NODE HEXAGONAL ELEMENTS

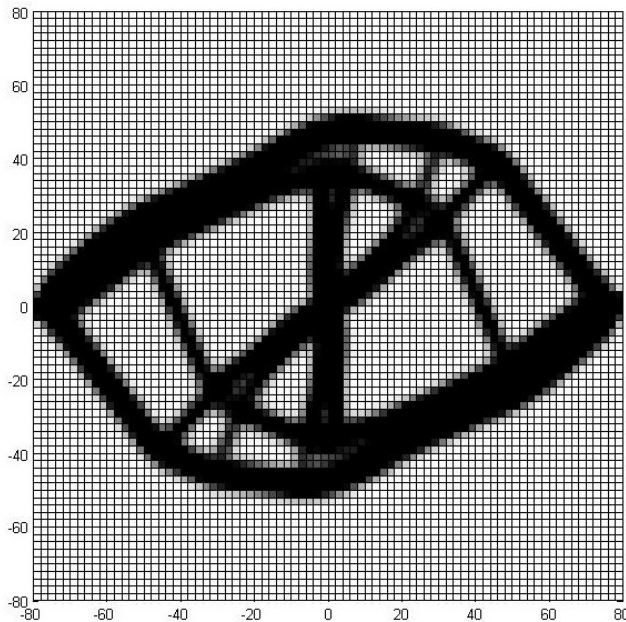


Figure 4.23. Four node square elements with filter; Volume 40%, $N = 80 \times 80$

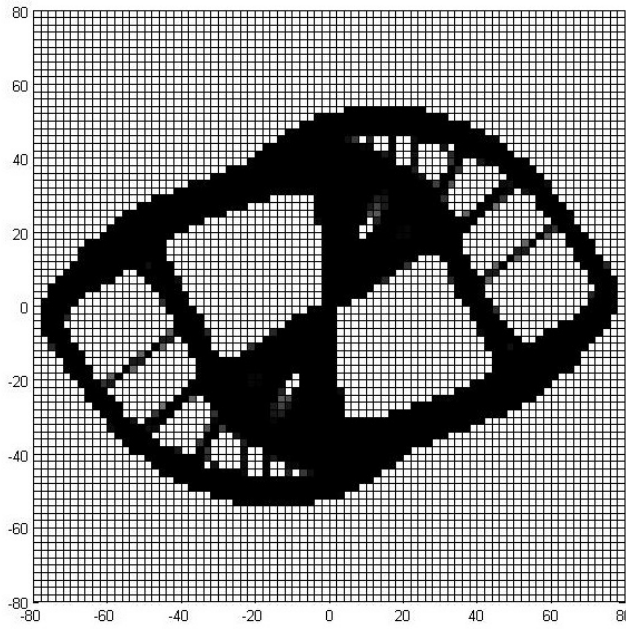


Figure 4.24. Nine node square elements; Volume 40%, $N = 80 \times 80$

4.7. ANOTHER LOAD CONDITION

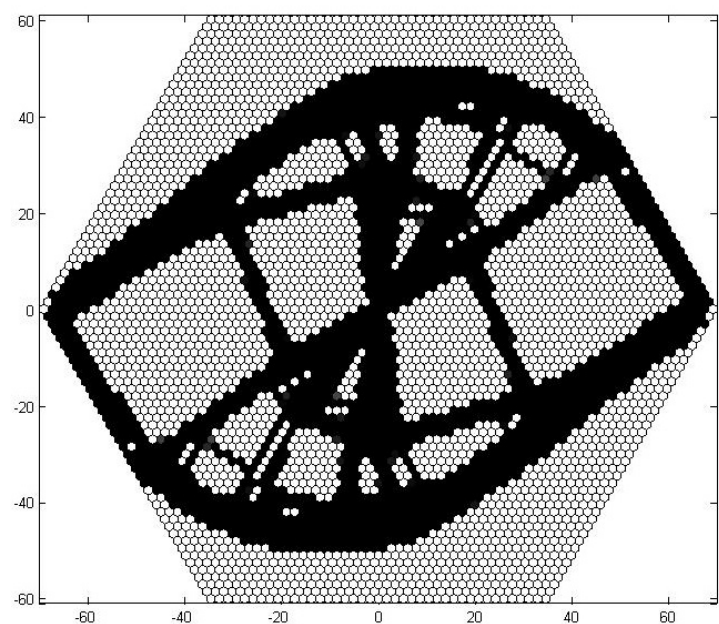


Figure 4.25. Six node hexagonal elements; Volume 40%, $N = 80 \times 80$

CHAPTER 4. FOUR NODE SQUARE ELEMENTS, NINE NODE SQUARE ELEMENTS AND SIX NODE HEXAGONAL ELEMENTS

Finite Elements	Filter	Number of iterations	Optimal solution / Black solution
Four node	No	42	1.7413
	Yes	177	1.7721
Nine node	No	54	1.6823
Six node	No	48	1.6130

Table 4.6. Volume 50%, Number of elements 80×80

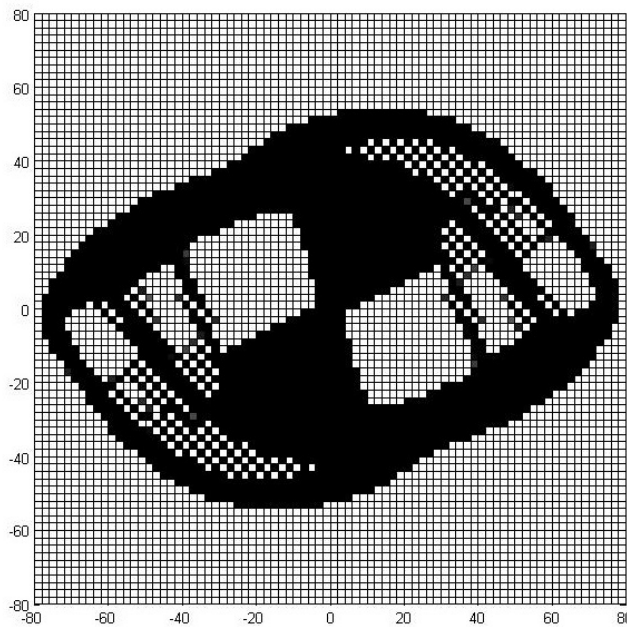


Figure 4.26. Four node square elements without filter; Volume 50%, $N = 80 \times 80$

4.7.2 50% Volume - 80×80

In Case of 50% volume the topology optimization problem is solved for all the three finite elements as shown in Figures (4.26, 4.27, 4.28, 4.29). The results obtained by solving topology optimization problem is shown in Table (4.6).

When topology optimization problem is solved for another load condition it is observed that for four node square elements checkerboard pattern appeared when it is solved without filter and is avoided by using filtration. Also in this case six nodes hexagonal elements works better than the nine node square elements and four

4.7. ANOTHER LOAD CONDITION

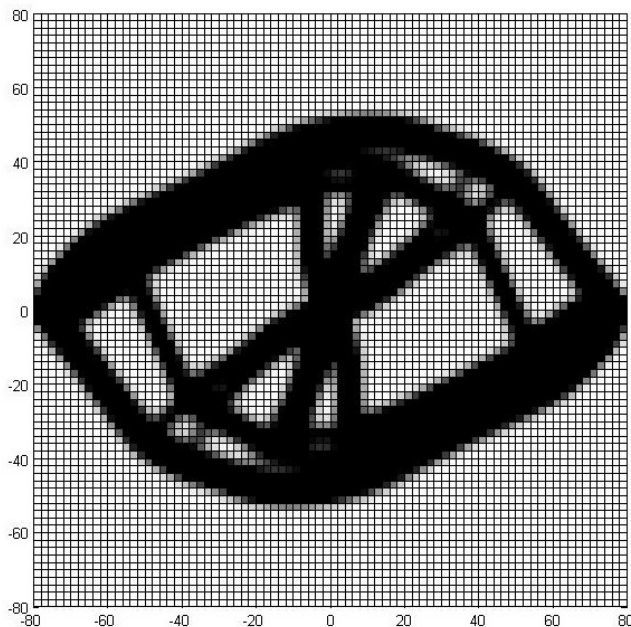


Figure 4.27. Four node square elements with filter; Volume 50%, $N = 80 \times 80$

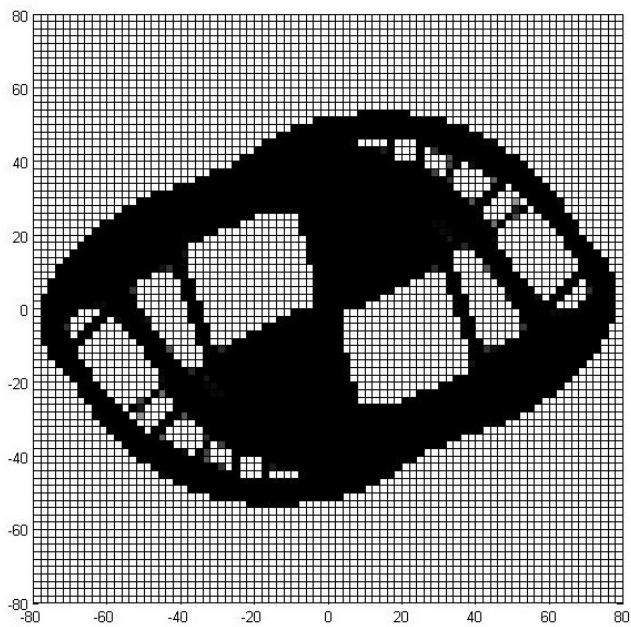


Figure 4.28. Nine node square elements; Volume 50%, $N = 80 \times 80$

CHAPTER 4. FOUR NODE SQUARE ELEMENTS, NINE NODE SQUARE ELEMENTS AND SIX NODE HEXAGONAL ELEMENTS

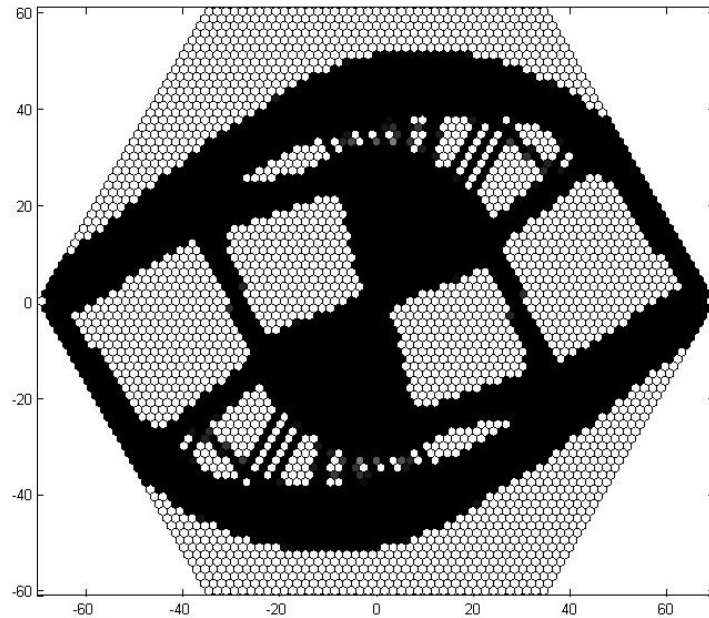


Figure 4.29. Six node hexagonal elements; Volume 50%, $N = 80 \times 80$

node square elements with filter. As it can be seen from the Tables (4.5) and (4.6) that the ratio of the compliance of obtained optimal solution by the compliance of obtained black solution is less for six nodes hexagonal elements. But for such loading conditions a lot of holes appeared in six node hexagonal elements and nine node square elements. One can use filtration to remove these holes, but we left it for future work. In terms of time computation nine node square elements are still very expensive as compared to other two finite elements. Six nodes hexagonal elements takes much computation time than four node square elements with filter.

Chapter 5

Conclusion and future work

In this thesis topology optimization problems for minimum compliance solved with SIMP approach for four node square elements with bilinear shape function, nine node square elements with quadratic shape function and six node hexagonal elements with Wachspress shape function.

5.1 Conclusion

The optimality techniques OC is compared with MMA solved for four node finite element with filter for three different topology optimization problems, namely half of the MBB beam, short cantilever beam and cantilever beam with a fixed hole. It is observed that MMA converge faster than OC but it takes much computation time per iteration. However, for such of kind of problems where a single constraint is involved OC works better and also by using gradient filtration technique the filtered derivatives are not exactly the correct derivatives and may be MMA is sensitive to this.

The topology optimization problems for minimum compliance are solved for alternate model and also with the same model but SIMP model objective function and compared the results obtained with SIMP model and also when it is solved with alternate model objective function. It is observed that in three studied topology optimization problems, the obtained structures are very similar for all scenarios but optimal value is slightly better for alternate model with SIMP model objective function.

CHAPTER 5. CONCLUSION AND FUTURE WORK

Finally, all the three finite elements are compared for SIMP model with MMA based optimizer. When the problem is solved with four node square elements without filter checkerboard pattern appeared in all the cases. As checkerboard pattern have artificially high stiffness, we use filtration. For nine node square elements and six node hexagonal elements no filtering is required as such and the resulting solid-void solution satisfies the imposed volume. But when the loading conditions are changed by tilting it, a number of holes are observed in the obtained structures of nine node square elements and six nodes hexagonal elements.

In all the cases six node hexagonal element with Wachspress shape functions give a better structure and optimized solution than the other finite elements. Nine node square elements is better than four node square elements with filter but it is very expensive in computation and use up more computation resources. As far as computation time is concern for six node hexagonal elements and four node square elements, six nodes takes more computation time than four node square elements with filter.

5.2 Recommendations for future work

Topology optimization for minimum compliance is solved with three different finite elements. Further studies however required to improve the convergence, using filtration in nine node square elements and six node hexagonal elements to remove the holes. One can also try to solve more technically interesting optimization problems. Four node square elements and nine node square elements may be extended to three-dimensional structures but six node hexagonal element is a challenge to do so.

Appendix A

Finite element method procedure

The Finite Element Method have following key steps in order to analyze solid bodies [11].

A.1 Domain discretization

The very first step is to divide the solid body into N_e elements. The procedure is called meshing, performed using pre-processor. The role of pre-processor is to generates unique numbers for all elements and nodes in a proper manner. An element is formed by connecting its nodes. All the elements together form the entire domain of the problem without any gap or overlapping. The density of mesh depends upon the accuracy required for analysis.

A.2 Displacement interpolation:

To make it convenient in formulating the FEM equations for elements, local coordinate system is used. Which is defined for an element in reference to the global coordinate system (A.2.1) that is defined for the entire structure. The displacement at points (x, y) within the element is a polynomial interpolation:

$$U^h(x, y) = \sum_{i=1}^{n_d} \mathbf{N}_i(x, y) \mathbf{d}_i = \mathbf{N}(x, y) \mathbf{d}_e \quad (\text{A.1})$$

where h is approximation, n_d is the number of nodes forming an element, \mathbf{d}_i is the unknown nodal displacement to be computed and expressed in a general form as $\mathbf{d}_i^T = \{\mathbf{d}_1^T, \mathbf{d}_2^T, \dots, \mathbf{d}_{n_f}^T\}$ where n_f is the number of degrees of freedom at a node.

APPENDIX A. FINITE ELEMENT METHOD PROCEDURE

And the vector \mathbf{d}_e is the displacement vector for the entire element, and has the form $\mathbf{d}_e^T = \{\mathbf{d}_1^T, \mathbf{d}_2^T, \dots, \mathbf{d}_{n_d}^T\}$. N is a matrix of shape functions for the nodes in the element.

A.2.1 Local and Global coordinates

Forces, displacements and stiffness matrices are often derived and defined for an axis system local to the member i.e. the coordinates apply to a single object. However there exist an overall axis system for the structure as a whole called global coordinate system or structure coordinate system i.e. the coordinates apply to everything uniformly [7].

A.3 Construction of shape function:

Construction of shape function depends on the geometry of the problem. Here 1-Dimensional case is explained but it can be extended to 2-Dimensional and 3-dimensional as well. Consider an element with n_d nodes at \mathbf{x}_i ($i = 1, 2, \dots, n_d$), for 1-Dimensional $\mathbf{x}^T = \{x\}$. The displacement component is approximated in the form of a linear combination of n_d linearly-independent basis functions $p_i(\mathbf{x})$.

$$u^h(\mathbf{x}) = \sum_{i=1}^{n_d} p_i(\mathbf{x}) \alpha_i = \mathbf{p}^T(\mathbf{x}) \alpha \quad (\text{A.2})$$

where u^h is the approximation of the displacement component, $p_i(\mathbf{x})$ is the basis function of monomials in the space coordinates \mathbf{x} , α_i is the coefficient for the monomial $p_i(\mathbf{x})$. The vector α is defined as:

$$\alpha^T = \{\alpha_1, \alpha_2, \dots, \alpha_{n_d}\}$$

The basis function $p_i(\mathbf{x})$ in Eq. (A.2) for 1-Dimensional has the form:

$$\mathbf{p}^T(\mathbf{x}) = \{1, x, x^2, x^3, \dots, x^p\}$$

The coefficient α_i in Eq. (A.2) can be calculated by solving Eq. (A.2) to be equal to the nodal displacements at the n_d nodes of the element. At node i it is of the following form:

$$d_i = \mathbf{p}^T(\mathbf{x}_i) \alpha \quad i = 1, 2, \dots, n_d$$

A.3. CONSTRUCTION OF SHAPE FUNCTION:

where d_i is the nodal value of u^h at $\mathbf{x} = \mathbf{x}_i$. It can be written in the matrix form as:

$$\mathbf{d}_e = \mathbf{P}\alpha \Rightarrow \alpha = \mathbf{P}^{-1}\mathbf{d}_e \quad (\text{A.3})$$

where \mathbf{d}_e is the vector that includes the values of the displacement component at all the n_d nodes in the element $\mathbf{d}_e^T = \{\mathbf{d}_1^T, \mathbf{d}_2^T, \dots, \mathbf{d}_{n_d}^T\}$. And \mathbf{P} is given by:

$$\mathbf{P} = \begin{bmatrix} \mathbf{p}^T(\mathbf{x}_1) \\ \mathbf{p}^T(\mathbf{x}_2) \\ \vdots \\ \mathbf{p}^T(\mathbf{x}_{n_d}) \end{bmatrix}$$

On substituting Eq. (A.3) into Eq. (A.2) gives shape functions as:

$$u^h(\mathbf{x}) = \sum_{i=1}^{n_d} N_i(\mathbf{x})d_i$$

or in the matrix form:

$$u^h(\mathbf{x}) = \mathbf{N}(\mathbf{x})\mathbf{d}_e$$

where $\mathbf{N}(\mathbf{x})$ is a matrix of shape functions defined as $\mathbf{N}(\mathbf{x}) = \mathbf{p}^T(\mathbf{x})\mathbf{P}^{-1}$.

A.3.1 Properties of shape function

The shape function $\mathbf{N}(\mathbf{x})$ have following properties:

1. Reproduction property and consistency
2. Linear independence
3. Delta function property

$$N_i(x_j, y_j) = \begin{cases} 1 & \text{for } i = j \\ 0 & \text{for } i \neq j \end{cases}$$

4. Partition of unity property

$$\sum_{i=1}^{n_d} N_i(\mathbf{x}) = 1$$

5. Linear field reproduction

$$\sum_{i=1}^{n_d} N_i(x)x_i = x$$

APPENDIX A. FINITE ELEMENT METHOD PROCEDURE

A.4 Formation of FE equations in local coordinate system

Finite Element equation for an element can be formulated by substituting the interpolation of the nodes, Eq. (A.1), and stain-displacement equation, $\varepsilon = \mathbf{L}\mathbf{U}$, where \mathbf{U} is the displacement vector ($\{u, v\}$) and \mathbf{L} is a matrix of partial differential operator into the strain energy equation:

$$\begin{aligned}\pi &= \frac{1}{2} \int_V \varepsilon^T \sigma \, dV = \frac{1}{2} \int_V \varepsilon^T \mathbf{c} \, \varepsilon \, dV \\ \pi &= \frac{1}{2} \int_{V_e} \varepsilon^T \mathbf{c} \, \varepsilon \, dV = \frac{1}{2} \int_{V_e} \mathbf{d}_e^T \mathbf{B}^T \mathbf{c} \, \mathbf{B} \, \mathbf{d}_e \, dV = \frac{1}{2} \mathbf{d}_e^T \left(\int_{V_e} \mathbf{B}^T \mathbf{c} \, \mathbf{B} \, dV \right) \mathbf{d}_e\end{aligned}$$

where e is stand for element and \mathbf{B} is called *strain matrix* defined as $\mathbf{B} = \mathbf{LN}$. Thus the strain matrix is calculated by use of shape functions as:

$$\mathbf{B} = \mathbf{LN} = \begin{bmatrix} \frac{\partial}{\partial x} & 0 \\ 0 & \frac{\partial}{\partial y} \\ \frac{\partial}{\partial y} & \frac{\partial}{\partial x} \end{bmatrix} \mathbf{N}$$

Once the strain matrix is calculated the stiffness matrix for solid can be found as:

$$\mathbf{k}_e = \int_{V_e} \mathbf{B}^T \mathbf{c} \, \mathbf{B} \, dV \quad (\text{A.4})$$

For bilinear rectangular element and hexagonal element stiffness matrix can be calculated by using Gauss Integration scheme see Appendix C.

Appendix B

Shape functions

One of the fundamental steps in a finite element analysis is the discretization of a continuous body containing infinite number of points in the surface into a discrete model with a limited number of points (or nodes) in the surface. The shape of the body between these nodes is approximated by functions. These functions are known as *shape functions*, and allow to relate the coordinates of every point of a finite element with the positions of its nodes and also relate the displacement of every point in an element with the displacement of its node. In two-dimensional elements shape function have natural coordinates (ξ, η) [8].

In our work the shape functions used for four node square elements, nine node square elements and six node hexagonal elements are bilinear shape functions, quadratic shape functions and Wachspress shape functions, respectively. These shape functions are as follows:

B.1 Four node square element

Shape functions for four node square elements are:

$$\begin{aligned} N1 &= (1/4) * (1 - \xi) * (1 - \eta); \\ N2 &= (1/4) * (1 + \xi) * (1 - \eta); \\ N3 &= (1/4) * (1 + \xi) * (1 + \eta); \\ N4 &= (1/4) * (1 - \xi) * (1 + \eta); \end{aligned} \tag{B.1}$$

B.2 Nine node square element

Shape functions for nine node square elements are:

$$\begin{aligned}
 N1 &= (1/4) * \xi * (1 - \xi) * \eta * (1 - \eta); \\
 N2 &= -(1/4) * \xi * (1 + \xi) * \eta * (1 - \eta); \\
 N3 &= (1/4) * \xi * (1 + \xi) * \eta * (1 + \eta); \\
 N4 &= -(1/4) * \xi * (1 - \xi) * \eta * (1 + \eta); \\
 N5 &= -(1/2) * (1 - \xi^2) * (1 - \eta) * \eta; \\
 N6 &= (1/2) * (1 + \xi) * (1 - \eta^2) * \xi; \\
 N7 &= (1/2) * (1 - \xi^2) * (1 + \eta) * \eta; \\
 N8 &= -(1/2) * \xi * (1 - \xi) * (1 - \eta^2); \\
 N9 &= (1 - \xi^2) * (1 - \eta^2);
 \end{aligned} \tag{B.2}$$

B.3 Six node hexagonal elements

Shape function for six node hexagonal elements are:

$$\begin{aligned}
 z &= (6 - 2 * \xi^2 - 2 * \eta^2); \\
 s &= 1/\sqrt{3}; \\
 N1 &= ((1 - 2 * s * \xi) * (1 - s * \xi + \eta) * (1 + s * \xi + \eta) * (1 + 2 * s * \xi)) / z; \\
 N2 &= ((1 - s * \xi + \eta) * (1 + s * \xi + \eta) * (1 + 2 * s * \xi) * (1 + s * \xi - \eta)) / z; \\
 N3 &= ((1 + s * \xi + \eta) * (1 + 2 * s * \xi) * (1 + s * \xi - \eta) * (1 - s * \xi - \eta)) / z; \\
 N4 &= ((1 + 2 * s * \xi) * (1 + s * \xi - \eta) * (1 - s * \xi - \eta) * (1 - 2 * s * \xi)) / z; \\
 N5 &= ((1 + s * \xi - \eta) * (1 - s * \xi - \eta) * (1 - 2 * s * \xi) * (1 - s * \xi + \eta)) / z; \\
 N6 &= ((1 - s * \xi - \eta) * (1 - 2 * s * \xi) * (1 - s * \xi + \eta) * (1 + s * \xi + \eta)) / z;
 \end{aligned} \tag{B.3}$$

Appendix C

Gauss integration

In finite element analysis the integration over the elements is an important step. Since the functions that are to be integrated over elements may be complex so it requires numerical treatment. In numerical integration over square elements the natural coordinates (ξ, η) ranges from +1 to -1 to enable the Gauss quadrature. *Gauss quadrature* is a numerical integration method over the elements in which the shape function is approximated by a polynomial expression which is exactly integrated [8].

C.1 Four node element and nine node element

For evaluation of integral (A.4) Gauss Integration scheme is used. For 1-dimensional integral it is evaluated at m *Gauss points* multiplied by corresponding *weight coefficients* as follows [11]:

$$I = \int_{-1}^{+1} f(\xi) d\xi = \sum_{j=1}^m w_j f(\xi_j)$$

Table (C.1) shows the locations of Gauss points and weight coefficients for different m . In general, the accuracy level for integration increases with the use of more Gauss points but excessive use of Gauss points will increase the computational time and it may not necessarily give better results. m Gauss points gives exact solution of polynomial integrand of upto an order of $n = 2m - 1$.

For 2-Dimensional integrations, the Gauss integration is sampled in two direc-

APPENDIX C. GAUSS INTEGRATION

m	Gauss Point ξ_j	Gauss Weight w_j	Accuracy order n
1	0	2	1
2	$-1/\sqrt{3}, 1/\sqrt{3}$	1, 1	3
3	$-\sqrt{0.6}, 0, \sqrt{0.6}$	5/9, 8/9, 5/9	5

Table C.1. Gauss integration points and weight coefficients for square elements

N	j	α_j	r_j	Gauss Weight w_j
1	0	0.0000000000000000	0.0000000000000000	0.255952380952381
	1	0.0000000000000000	0.748331477354788	0.124007936507936

Table C.2. Quadrature parameters

tions, as follows:

$$I = \int_{-1}^{+1} \int_{-1}^{+1} f(\xi, \eta) d\xi d\eta = \sum_{i=1}^{n_x} \sum_{j=1}^{n_y} w_i w_j f(\xi_i, \eta_j)$$

C.2 Six node element

For numerical integration, fully symmetric quadrature rules are developed for regions with regular hexagonal symmetry [26]. The quadrature rule is invariant under 60° rotation as shown in the Figure (C.1) and expressed as:

$$\int_{\Omega_e} f d\Omega \approx w_0 f(0,0) + \sum_{j=1}^N \sum_{i=1}^6 w_j f\left(r_j, \alpha_j + \frac{\pi i}{3}\right)$$

Here w_j represents weight corresponding to the quadrature point at distance r_j from the origin and angle $\alpha_j + \frac{\pi i}{3}$ from the horizontal axis for each $1 \leq i \leq 6$. The list of quadrature points for various values of j can be found in the Table (C.2). In order to have a complete list of quadrature rule for Wachspress hexagonal element used by Lyness JN and Monegato G [12]; see Talischi C; Paulino GH and Le CH [26]; article. The Gauss integration points used for six node and the center of the hexagonal element are shown in Table (C.3).

C.2. SIX NODE ELEMENT

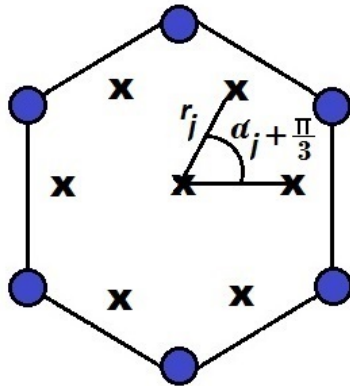


Figure C.1. Schematic illustration of the quadrature rule for the regular hexagonal element: integration points are shown by "x" marks

m	Gauss Point x-coordinate	Gauss Point y-coordinate	Gauss Weight w_j
1	0	0	0.255952380952381
2	$\sqrt{0.56} * 1$	$\sqrt{0.56} * 0$	0.124007936507936
3	$\sqrt{0.56} * 1/2$	$\sqrt{0.56} * \sqrt{3}/2$	0.124007936507936
4	$\sqrt{0.56} * -1/2$	$\sqrt{0.56} * \sqrt{3}/2$	0.124007936507936
5	$\sqrt{0.56} * -1$	$\sqrt{0.56} * 0$	0.124007936507936
6	$\sqrt{0.56} * -1/2$	$\sqrt{0.56} * -\sqrt{3}/2$	0.124007936507936
7	$\sqrt{0.56} * 1/2$	$\sqrt{0.56} * -\sqrt{3}/2$	0.124007936507936

Table C.3. Gauss integration points for hexagonal element and weight coefficients

Appendix D

Hexagonal element

A hexagon is a polygon with six edges and six vertices. In this Thesis a regular hexagon takes into consideration in which all the sides are of same length and all internal angles are 120 degrees. A local *natural coordinate system* (ξ, η) is defined for hexagonal element with its origin located at the center of the element. The coordinates for 6 nodes are shown in Figure (D.1). The local node numbering is also shown in it.

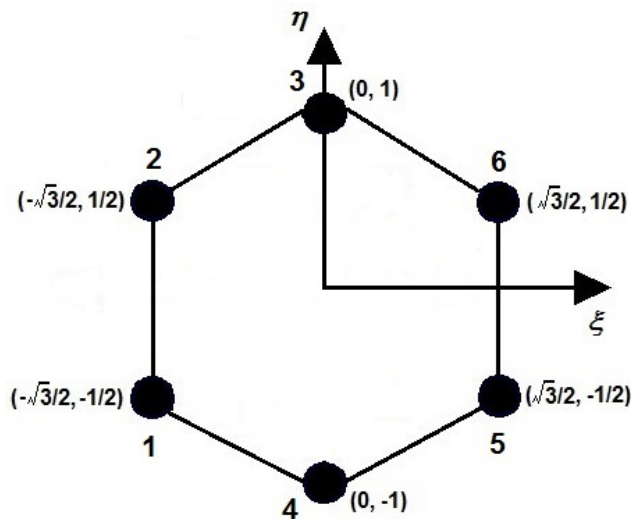


Figure D.1. Coordinates for hexagonal element

APPENDIX D. HEXAGONAL ELEMENT

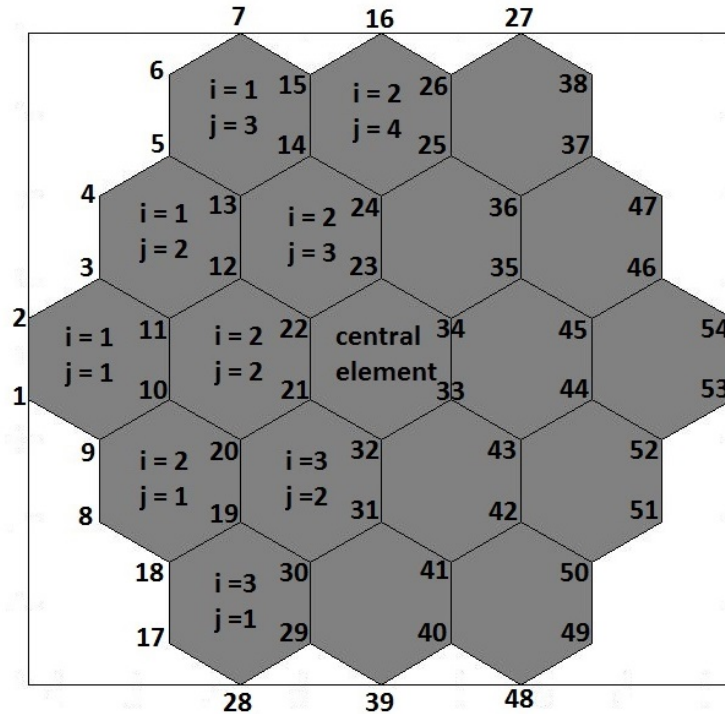


Figure D.2. Six node hexagonal elements; $N = 2 \times 2$

The elements are numbered by taking horizontal and vertical components in diagonal as shown in Figure (D.2) where central element have coordinates $(0, 0)$. The nodes are also numbered in the Figure. Due to symmetry, half portion of the finite element is calculated and the other is found by using that knowledge.

Bibliography

- [1] Bendsøe MP. Optimal shape using a dual method with discrete variables. *Structural Optimization*, 17: 14-24, 1989.
- [2] Bendsøe MP. *Optimization of structural topology, shape and material*. Berlin, Heidelberg, New York: Springer, 1995.
- [3] Bendøse MP; Kikuchi N. Generating optimal topologies in optimal design using a homogenization method. *Comp. Meth. Appl. Mech. Engrg*, 71: 197-224, 1988.
- [4] Bendsøe MP; Sigmund O. *Topology optimization, theory, methods and applications*. Springer-Verlag Berlin Heidelberg, 2003.
- [5] Chapman CD. Structural topology optimization via the genetic algorithm. Massachusetts Institute of Technology, 1994.
- [6] Diaz AR; Sigmund O. Checkerboard patterns in layout optimization. *Structural Optimization*, 10(1): 40-45, 1995.
- [7] Dr. Caprani C. Structural Dynamics 4th Year *Structural Engineering*, 2009/10.
- [8] <http://fea4noobs.wordpress.com/chapter-index/>
- [9] Jog C; Haber R. Stability of finite element models for distributed-parameter optimization and topology design. *Comp. Meth. Appl. Mech. Engrg*, 130(3-4): 203-226, 1996.
- [10] Langelaar M. The use of convex uniform honeycomb tessellations in structural topology optimization. Proceedings of the 7th world congress on structural and multidisciplinary optimization, Seoul, South Korea, 21-25 May, 2007.
- [11] Liu GR; Quek SS. The finite element method - A practical course. Elsevier Science Ltd, Great Britain, MPG Books Ltd, Bodmin, Cornwall, 2003.

BIBLIOGRAPHY

- [12] Lyness JN; Monegato G. Quadrature rules for regions having regular hexagonal symmetry. *SIAM J Numer Anal*, 14(2): 283-295, 1977.
- [13] Meijboom M. Topology optimization of dynamic problems. Report External Traineeship. Reportnr.: DCT.2003.108, Id. Nr.: 448220. Eindhoven, 2003.
- [14] Mlejnek HP. Some aspects of the genesis of structures. *Struct. Multidisc. Optim*, 5: 65-69, 1992.
- [15] Nguyen VT. Finite element simulation of Durelli's photoelastic stress minimization method for shape optimization. Victoria University of Technology, Australia, 1999.
- [16] Rouhi M. Topology optimization of continuum structures using element exchange method. Mississippi State, Mississippi, May, 2009.
- [17] Rozvany GIN; Zhou M; Gollub. Continuum-type optimality criteria methods for large finite element systems with a displacement constraint. 2(2): 77-104, 1990.
- [18] Saxena R; Saxena A. On honeycomb representation and SIGMOID material assignment in optimal topology synthesis of compliant mechanism. *Finite Elem Anal Des*, 43: 1082-1098, 2007.
- [19] Sigmund O. A 99 line topology optimization code written in Matlab. *Struct. Multidisc. Optim*, 21: 120-127, 2001.
- [20] Sigmund O; Petersson J. Numerical instabilities in topology optimization: A survey on procedures dealing with checkerboards, mesh-dependencies and local minima. *Structural Optimization*, 16(1): 68-75, 1998.
- [21] Stolpe M; Svanberg K. An alternative interpolation scheme for minimum compliance topology optimization. *Struct Multidisc Optim*, 22: 116-124, Springer-Verlag, 2001.
- [22] Stolpe M; Svanberg K. On the trajectories of penalization methods for topology optimization. *Struct. Multidisc. Optim*, 21: 140-151, 2001.
- [23] Sukumar N; Malsch EA. Recent advances in the construction of polygonal finite element interpolants. *Arch Comput Methods Eng*, 11: 1-38, 2005.

- [24] Svanberg K. The Method of moving asymptotes - a new method for structural optimization. *Int. J. Numer. Mech. Eng.*, Vol.24: 359-373, 1987.
- [25] Svanberg K. A primal-dual interior-point method for the MMA subproblem, 2009.
- [26] Talischi C; Paulino GH; Le CH. Honeycomb Wachspress finite elements for structural topology optimization. *Struct. Multidisc. Optim.*, 37: 569-583, 2009.
- [27] Wachspress EL. A rational finite element basis. Academic Press, New York, 1975.
- [28] Warren J. On the uniqueness of barycentric coordinates. Contemporary mathematics: proceedings of AGGM'02, pp 93-99, 2003.
- [29] Werme M. On methods for discrete topology optimization of continuum structures. Royal Institute of Technology, Sweden, 2008.
- [30] Zhou M; Rozvany GIN. The COC algorithm, part II: Topological, geometry and generalized shape optimization. *Comp. Meth. Appl. Mech. Engrng*, 89: 197-224, 1991.

TRITA-MAT-E 2013:35
ISRN-KTH/MAT/E—13/35-SE